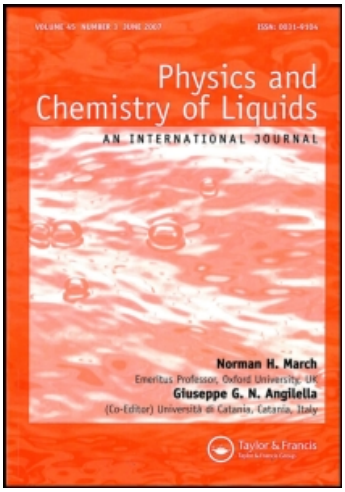

Physics and Chemistry of Liquids

Publication details, including instructions for authors and subscription information:
http://www.informaworld.com/smpp/title~content=t713646857

Review of Mesoscopic Modeling of Liquids in Materials Science

A. Ten Bosch[a]
[a] Laboratoire de Physique de la Matière Condensée, CNRS, Nice Cedex 2, France

Online publication date: 27 October 2010

Physics and Chemistry of Liquids
Vol. 41, No. 5, October 2003, pp. 441–474

Taylor & Francis
Taylor & Francis Group

Review

MESOSCOPIC MODELING OF LIQUIDS IN MATERIALS SCIENCE

A. TEN BOSCH*

Laboratoire de Physique de la Matière Condensée, CNRS 6622 Parc Valrose, 06108 Nice Cedex 2, France

(Received 16 April 2003)

Mesoscopic theories can be used in the field of materials science to derive local average properties of relevance to the engineer such as flux, pressure, average density or composition. In the following density functional theory will be described and applied to different systems of interest and in particular, to materials formed from complex liquids as characterized by atomic structure and the type of interaction between the individual particles. The calculation of the solid to liquid transition will be explained in detail as a prototype for other order disorder transitions. The theory of polymers in solution will be revisited and used to calculate phase separation in mixtures. An extension of the theory to include the orientation of rodlike, long molecules will be applied to liquid crystals. In the presence of an interface, the system properties depend strongly on position in space and can be predicted from parameters obtained in the bulk in a square gradient approximation for sufficiently smooth and small deviations from the uniform distribution. A phase transition is often used to prepare heterogeneous materials by nucleation and growth. It will be shown how the equilibrium theory can be extended to study the dynamics of nonequilibrium phenomena.

Keywords: Complex liquids; Order–disorder transitions; Polymers in solution; Liquid crystals

*E-mail: tenbosch@unice.fr

ISSN 0031-9104 print: ISSN 1029-0451 online © 2003 Taylor & Francis Ltd
DOI: 10.1080/0031910031000155461

1. INTRODUCTION

1.1. Applications

Materials research is very old, for progress has always required new materials to fulfill new needs. However, the engineers that conceive new technologies often prefer to choose well-established and well-known materials to avoid the risks and costs of advanced new developments, although thus also losing the advantages. Often obsolete materials slow down the introduction of a new and better application. On average, 10–20 years are needed to bring a material from the laboratory to large commercial use. Companies are conservative and do not wish to use what they do not know. The future belongs to those who can accelerate the acceptance of the innovations currently proposed by scientists and basic research plays a role. The path from conception to commercialization is long. Along with experimentation to prepare and characterize a new material, more and more modeling and simulation is being used. Theory can help save time and money by reducing the need for extensive selection, testing and trials. Often the information needed does not require a full scale atomistic treatment. The idea is rather to reach a reasonably accurate result within a reasonable cost and time. To this purpose *mesoscopic* models can be applied to derive local average properties of relevance to the engineer such as flux, pressure, composition. In the following one such theory will be described and applied to different systems of interest in the field of materials science. The mathematics will be kept to a minimum and the emphasis placed on the basic concepts and results. The article is intended as an introduction to an active field for the nonspecialist in research and industry and for graduate students interested in materials science.

1.2. An Overview

Many new materials are prepared starting from the liquid state of what are called *complex* liquids. Some examples of *complex liquids* are liquid metals, polymer melts and solutions, or on a larger scale, emulsions and suspensions. The reasons why a

fluid qualifies as complex are found in the atomic structure and the type of interaction between the individual particles.

One of the first tests of a statistical theory (and a stringent one) has been the calculation of the temperature and density at which a complex fluid will solidify. The calculation of the *solid to liquid transition* will be explained in detail as a prototype for other order–disorder transitions.

It is not always possible to obtain true mixtures especially in materials consisting of chainlike molecules. The Flory theory of *polymers* in solution was developed over 50 years ago and is still being used. The classic theory will be revisited and used to calculate the phase diagram and the change in the polymer conformation due to the effect of the solvent.

Liquid crystals and more recently liquid crystal polymers and elastomers require an extension of the theory to rodlike or long molecules. These systems are in the liquid phase but show ordering of the relative orientation of the molecules.

The properties of the solid–liquid or liquid–liquid interface play a role in the stability of heterogeneous materials, in the preparation of composites, in the alignment of liquid crystals in devices. In the presence of an *interface*, the system properties depend strongly on position in space and can be predicted from parameters obtained in the bulk. A *square gradient approximation* is introduced for sufficiently smooth and small deviations from the uniform distribution.

The transition from the liquid to the solid or from the liquid to the vapor is a typical *nucleation and growth* phenomenon. The dynamics of the phase transition are often used to prepare heterogeneous materials with clusters or films of one type of material embedded in another. It will be shown how the equilibrium theory can be extended to nonequilibrium phenomena.

Each chapter will be illustrated by an industrial example of the fundamental problems which occur and the method with which they can be approached.

1.3. Why Density Functional Theory?

The equilibrium theory presented here is most often denoted *density functional theory* or simply DFT (Löwen, 1994). The idea is that average system properties will all follow as functions of the probability density or particle number density n which measures where to find a particle of the system at a given point in space and at a given time. In equilibrium, the most probable value for n is calculated by minimization of a relevant functional such as the free energy. The theory that results

– can be used to compare systems by a simple change of parameters
– can be used to test simple model potentials
– can give a basis for empirical laws
– justifies the widely used (Landau) expansions of thermodynamic potentials and refines these types of theories
– can predict new phases (crystal structure, glasses)
– can be applied to many different materials (metals, polymers, liquid crystals)
– can be extended to nonuniform systems such as crystals or surfaces
– can be extended to dynamic systems.

The parameter which determines the properties of the material is the interparticle potential. The exact form of the interaction between two different particles is rarely

known to any accuracy. Over the years, model potentials have been developed, refined and applied to the calculation of system properties. Numerical simulation studies and experimental results have been used to test a given model. The first step in the theory is the choice of interparticle potential.

1.4. The Model Potential

A material consists of particles which can be atoms, molecules or groups of these and which interact through different types of forces. Modeling requires a definition of the structure of the particles and the resulting interaction (Isrealachvili, 1992). Some time-tested examples are:

– Atomic materials made up of individual atoms of a spherical form without strong chemical binding. The effective interaction between atoms shows a repulsion at short distance between two atoms mainly due to the impossibility of overlap of atomic electron shells. At larger separation, atoms must attract each other. A typical effective interaction potential is given in Fig. 1.

The simplest systems are made up of rare gas atoms. These have been successfully modeled by Lennard Jones (12-6) potentials. The repulsive interaction is assumed to follow a $1/r^{12}$ decay. The attraction arises mainly from Van der Waals forces due to an induced dipole moment formed on one atom by shifting of the electronic change due to the presence of the other and decays as $1/r^6$. Two parameters are needed: the distance a which fixes the minimum at $(2)^{1/6}\ a$ and the energy ε which fixes the lowest energy. The potential is then $V(r) = \varepsilon[(a/r)^{12} - (a/r)^6]$.

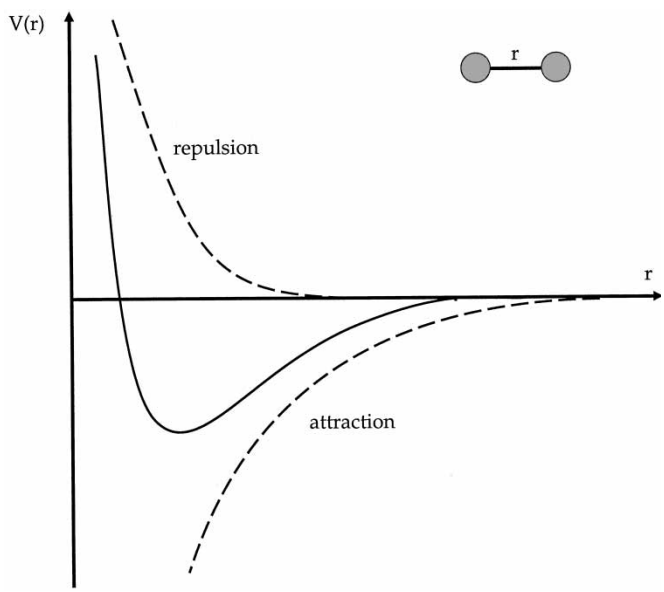

FIGURE 1 The interaction potential $V(r)$ between two spherical particles as a function of distance r with repulsion at short and attraction at large separation.

These model systems are extensively used as a first step in testing new theories and can be applied to most materials by astute adjustment of parameters.

– Often the effect of the attraction is minor and the repulsion strong. Such systems can be usefully modeled by "hard spheres" with

$$V(r) = \infty \quad (r < a)$$
$$= 0 \quad (r > a)$$

All information is contained in the single parameter a and analytical calculations are simple to do. The disadvantage is that temperature dependence cannot be studied due to a Boltzman factor of 0 or 1. For this reason a perturbation calculated in the attractive potential is often a useful path.

– In metals and semi-conductors the presence of electrons will be important and usually requires quantum mechanics. A first idea of their properties can be obtained from classical model potential calculations and quantum mechanic effects are included with the help of an effective potential (Foiles, 1996).
– Charged particles are found in electrolytes and atomic plasmas with additional long range Coulomb ($V(r) \propto 1/r$) or screened Coulomb interactions ($V(r) \propto \exp(-r/\xi)/r$).
– If the form of the particles of the fluid is not spherical, the potential will depend also on the angle of the particle axis, as has been shown for Van der Waals interactions and hard core interactions between ellipsoids or rods. Liquid crystals fall into this group. The molecules of liquid crystalline fluids are elongated and are usually modeled by rods (albeit sometimes of infinitely small width).
– Flexibility towards deformation of the molecules becomes important in long molecules and polymers. An elastic Hooke type interaction between the monomers which is simply proportional to the deformation is then used. The three types of possible deformations of the monomer bond are elongation, bend away from the preferred direction and torsion (Yamakawa, 1971).

In the spirit of coarse graining, interactions balance within a certain length scale and details of atomistic structure do not play a role in large scale phenomena. The model interactions of atomic systems and DFT have also been applied with success to the larger size scale of colloidal systems: suspensions (s/l), emulsions (l/l), aerosols (s/g) and foams (g/l).

Once the model interaction has been chosen, the DFT theory provides a method to calculate the *phase diagram* of the material, the simplest of which is the well-known pressure–temperature or temperature–density relation of pure materials. In the solid, the crystal structure can change with temperature. Sometimes materials are prepared from two or more components that mix or not. In mixtures or in the presence of impurities the phase diagram and the gas, liquid or solid transitions depend on the proportion of each component. Complex phase diagrams occur as can be seen for metal alloys (Ohring, 1992). An example is given in Fig. 2.

Liquid crystal systems show an orientational order of the molecular axis. Molecules align parallel in the nematic phase, helicoidal in the cholesteric, in layers in the smectic etc. An example of phase diagram is given in Fig. 3.

Phase diagrams can be measured or derived from atomistic numerical simulation and provide a good test for the hypotheses of a theory. In the next chapter, calculation of the solid–liquid transition based on DFT is explained.

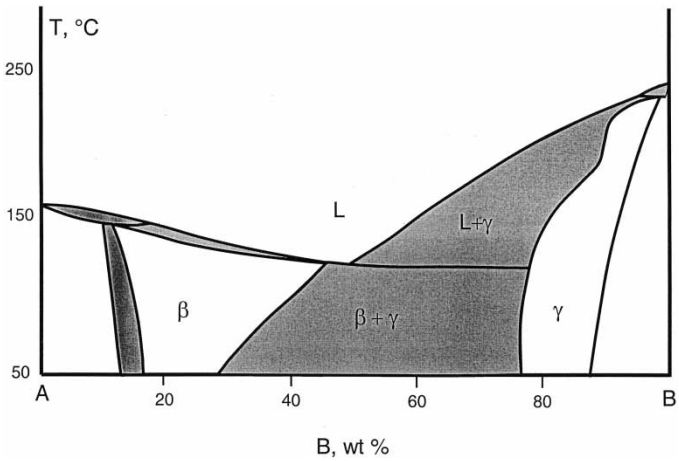

FIGURE 2 Phase diagram in a mixture of A and B: temperature T as a function of weight concentration of B for $L =$ liquid phase, β and γ crystal phases. Biphasic zones are shaded.

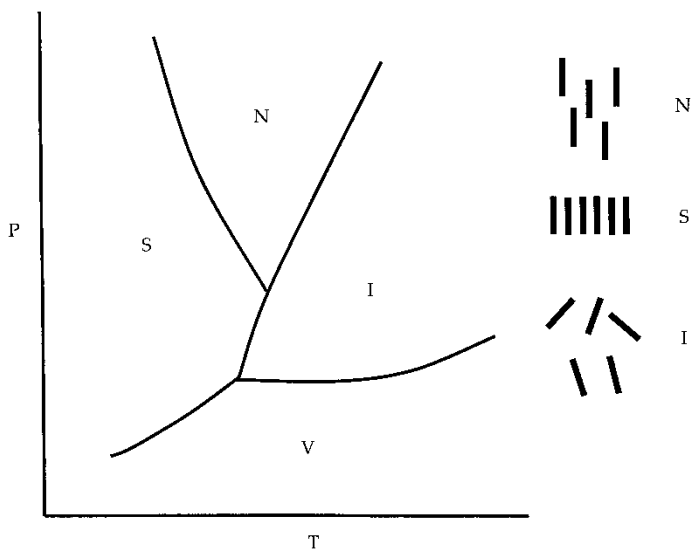

FIGURE 3 Phase diagram of a liquid crystal: pressure P, temperature T for the liquid nematic N, smectic S and isotropic I phases and vapour phase V.

2. THE SOLID–LIQUID TRANSITION

2.1. Introduction

The different behavior of a solid and a liquid is considered to be due to the fact that in a solid the particles are bound to the crystalline sites whereas in a liquid, free motion between sites is possible. The glassy state is an intermediate metastable phase of aperiodic crystal. Phenomenological criteria have been found.

1. The Lindeman criterion states that a solid will melt when the mean thermal vibration amplitude of the particles on a crystalline site becomes larger than 17–19% of the lattice dimension. Although a dynamic criterion, the average distribution of atoms on crystal sites in DFT does not depend on time and provides a measure for the Lindeman parameter.
2. The Hansen Verlet criterion states that a liquid will crystallize when the nearest neighbor order reaches a critical value. The structure factor $S(q)$ is the Fourier transformation of the correlation between two atoms of the fluid, which depends uniquely on the density and the interaction and can be calculated in DFT. Empirically, the critical value of $S(q)$ has been found to lie near 0.8.

Phase diagrams are determined in experiment by plotting a physical characteristic of the system that is known to change at the phase transition. The specific heat measured in a calorimetric setup is one example and a typical curve is shown in Fig. 4. Phase transitions can also be monitored by

– Thermodynamic properties such as the density, the density correlation function or structure factor, the compressibility, the concentration.
– Nonequilibrium properties such as diffusion coefficient, viscosity

The phase diagram of a system is extremely important in applications. For example, in order to study genome sequences, DNA polymers must be crystallized. As this does not always occur, hundreds of samples must be handled at a time. The phase diagram also defines the range of usefulness of a given material. The metal alloy used in a bridge should not melt, change crystal structure or show segregation in the range of temperature to which it will be exposed. The required range of temperatures determines the material which will ultimately be used and is very sensitive to impurities. If stability

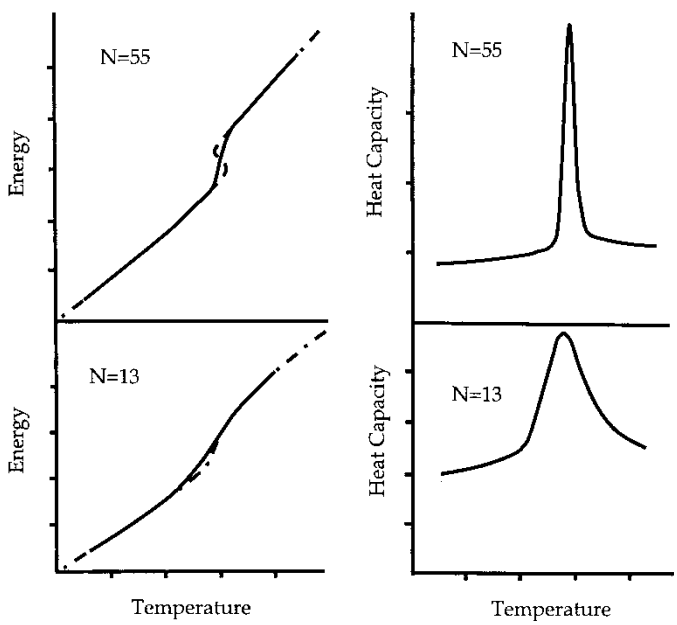

FIGURE 4 The solid to liquid melting transition in a cluster of N atoms with size effect on the change of the internal energy and the heat capacity at the transition (Labastie and Whetten, 1990).

to high temperatures is required, additional components can be added and the phase diagram replotted. Some direction can be given by theory. The theory should give trends as a function of parameters of the system, such as for example the density and the type of interactions present. It has been found that

– the number density n of a system is a parameter which can be used to calculate other useful thermodynamic and some nonequilibrium properties
– the most probable thermodynamic functional $\Omega(n, T, V, \mu)$ will be an optimum for the equilibrium density in a given set of external conditions: temperature T, volume V, chemical potential μ.

The method proceeds therefore to find an appropriate expression for the pressure or free energy as a function of the density and then to use a variational principal in order to obtain an equation for n. The solution of the equation leads to various values of $n(T, V, \mu)$ which must be checked for stability and relevance in order to eliminate the nonphysical solutions. If one solution remains, the system is in an uniform phase of that density. If two or more solutions are found, coexistence of different phases of different density may occur.

2.2. The Method

As an example, the DFT method for calculation of the solid–liquid transition of a Lennard Jones fluid is sketched in recipe form (Singh, 1991).

(1) How to choose the function to minimize?
In the thermodynamic limit the results will be independent of the ensemble chosen. (This will not be true for the finite systems often the object of molecular simulations.) The thermodynamic ensemble most often used is temperature T, volume V and chemical potential μ so that the function of interest is the grand canonical potential $\Omega(T, V, \mu) = -pV$ (p is the pressure). It can be shown that the difference of the actual thermodynamic function $\Omega_0(T, V, \mu)$ and the functional $\Omega(T, V, \mu(n))$ for a given density n is always positive. Therefore the equilibrium density n^* minimizes the functional and the variational principal is $\delta\Omega/\delta n\ (T,V,\mu(n)) = 0$ for $n = n^*$. It is often simpler to determine the free energy functional F defined as $\Omega(T, V, \mu(n)) = F(T, V, \mu(n)) - \mu N(T, V, \mu(n))$ for a total number of particles $N(T, V, \mu(n))$.

(2) How to express the free energy functional?
For an ideal gas without interactions between atoms of mass m, only the entropy contributes and

$$F_{\mathrm{id}} = kT \int_V d\boldsymbol{r} n(\boldsymbol{r})(\ln n(\boldsymbol{r})\Lambda - 1) \quad \text{with } \Lambda = (h/(2\pi mkT)^{1/2})^3$$

In a system with interactions, $F = F_{\mathrm{id}} + F_{\mathrm{ex}}$. The excess free energy F_{ex} is written as a (functional) expansion in a reference system of density n_0.

$$F_{\mathrm{ex}} = F_0 + \int_V d\boldsymbol{r}(n(\boldsymbol{r}) - n_0)\frac{\delta F_{\mathrm{ex}}}{\delta n(\boldsymbol{r})}\bigg|_{n=n_0} + \frac{1}{2}\int d\boldsymbol{r}d\boldsymbol{r}'(n(\boldsymbol{r}) - n_0)(n(\boldsymbol{r}') - n_0)\frac{\delta^2 F_{\mathrm{ex}}}{\delta n(\boldsymbol{r})\delta n(\boldsymbol{r}')}\bigg|_{n=n_0} + \cdots$$

The first term in the expansion is the constant excess energy of the reference system. The second term is the renormalization of the chemical potential by the interatomic

interactions which induce an effective uniform mean field

$$c^{(1)}(r; n_0) = -\frac{1}{kT}\frac{\delta F_{\text{ex}}}{\delta n(r)}\bigg|_{n=n_0}$$

The third term introduces the direct correlation function which is a measure of the position dependence of the average interaction between atoms (Frisch and Lebowitz, 1964):

$$c^{(2)}(r, r'; n_0) = -\frac{1}{kT}\frac{\delta^2 F_{\text{ex}}}{\delta n(r)\delta n(r')}\bigg|_{n=n_0}$$

(3) How to include the interaction?
The hard sphere system is used as a reference for which $c^{(2)}(r)$ is a known function. $c^{(2)}_{\text{HS}}(r)$ (Fig. 5). For the Lennard Jones potential, the repulsive interaction at short interatomic distance is replaced by the hard sphere potential and the direct correlation function becomes an expansion in the attractive interaction $\varphi(r)$: $c^{(2)}(r) = c^{(2)}_{\text{HS}}(r) + \Delta\ c^{(2)}(r)$. Usually, $\Delta c^{(2)}(r)$ is replaced by the weak attractive interaction for $r > a$, $\Delta c^{(2)}(r) = -\varphi(r)/kT$.

(4) How to simplify the problem, and accelerate the calculations?
An appropriate ansatz for the density functional is made which introduces one or more parameters. The functional $\Omega(T, V, \mu(n))$ or free energy functional $F(T, V, \mu(n))$ then become a function of these parameters. The minimization procedure becomes a calculation of simple derivatives in the parameters.

A useful expression for the present problem is

$$n(r) = (\alpha/\pi)^{3/2} \sum_{\boldsymbol{R}_n} \exp(-\alpha(\boldsymbol{r} - \boldsymbol{R}_n)^2)$$

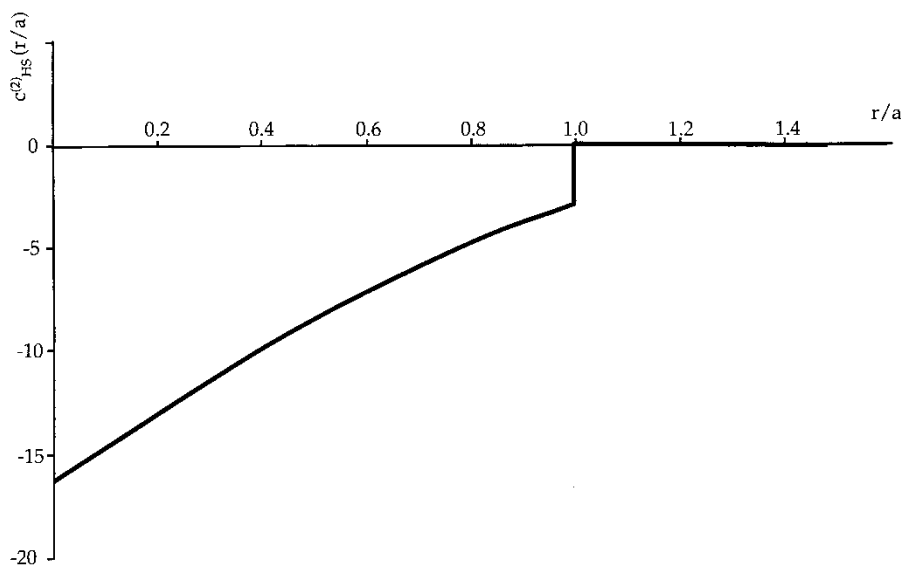

FIGURE 5 The hard sphere direct correlation function $c^{(2)}_{\text{HS}}(r/a)$ for hard sphere radius a, packing fraction 0.35.

This function can be used to describe the density in the crystal of crystal lattice vectors $\mathbf{R}_n$. The atoms have a finite probability to be centered in $\mathbf{R}_n$ as measured by α. In the liquid $\alpha = 0$ and the density is uniform. At the transition from solid to liquid, at least two solutions for $\alpha = 0$ and $\alpha > 0$ exist.

The parameter α defines the vibrational amplitude of the atoms which is a measure of localization on crystalline site and thus a decreasing function of temperature.

(5) How to calculate the density?
For a given average density $\tilde{n}$, the ansatz for $n(r)$ is inserted in $\Omega(T, V, \mu(n))$ to obtain a function $\Omega(T, V, \alpha)$ which is derived in α to find the minima $\delta\Omega/\delta\alpha = 0$. The resulting equation for α is solved, usually requiring a numerical procedure.

(6) How to eliminate spurious solutions?
The physical solution or solutions are found from $\Omega(T, V, \alpha)$ as the values α^* for which $\Omega(T, V, \alpha^*) < \Omega(T, V, \alpha_i)$ for all other α_i.

(7) How to include supplementary conditions?
It is sometimes useful to introduce the fixed number of particles $N = \int_V d\mathbf{r}\, n(r)$ as a supplementary condition for the variation. In a perfect crystal, a fixed number of atoms N_c in the crystal cell V_c is also used. $N_c = \int_{V_c} d\mathbf{r}\, n(r)$. These conditions help to eliminate spurious solutions and therefore accelerate the calculations.

(8) How to find the liquid–solid transition at given T, V, μ?
If a real solution for α is found, then $n(r)$ is defined and one phase of that average density $\tilde{n}$ is possible. The resulting functional $\Omega(T, V, \alpha(\tilde{n}), \tilde{n})$ is now minimized with respect to $\tilde{n}$. If many solutions are found, some may be eliminated by choosing the lowest value of Ω. If two solutions with equal values of Ω are found at a given temperature, then this is the transition temperature for melting or crystallization, as derived from thermodynamic stability and therefore the limiting temperature for the transition. Hysteresis from supercooling or superheating is due to dynamic effects and not obtained in this method. Similarly three coexisting phases (3 different values of the set $(\alpha, \tilde{n})$ for equal Ω which fulfill all supplementary conditions) are found at the triple point. Note that metastable phases which are relative minima of Ω can exist over a finite temperature range (Fig. 6).

For the Lennard Jones system, the resulting phase diagram from DFT is shown in Fig. 7. The well-known scaling laws in kT/ε and $\tilde{n}a^3$ are automatically obtained. The comparison to experiment is satisfactory. An application of the phase diagram is use of rare gas vapor to prevent metal evaporation in light bulbs (halogen lamps).

At the phase transition, the empirical laws have been verified. The Lindeman parameter depends on the parameters of the model and varies between 0.07 and 0.15.

(9) To what other systems can this method be applied?
Rare gases are ideally adapted for use as test systems for the theory (Rice and Gray, 1965) and the results are satisfying. By adjusting the parameters ε, and a, application to any system without strong chemical or electrical forces is possible as a good first approximation. Examples of calculated phase diagrams using other model potentials (Yukawa suspensions and plasmas, hard spheres, molecular liquids, metals) are given in Singh (1991).

The limits and extensions of the method are still being explored. In principal, the theory is applicable and allows for "rapid" calculation and comparison of phase

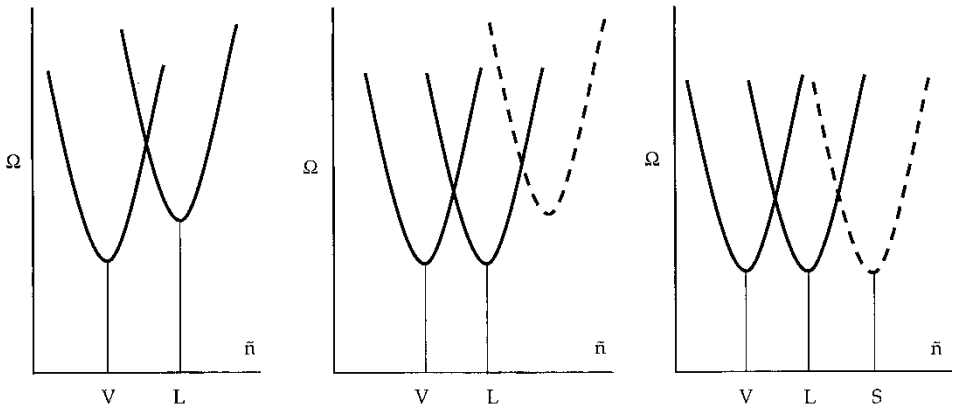

FIGURE 6 The thermodynamic potential Ω as a function of average density $\tilde{n}$ and crystallinity α: $\alpha = 0$ (solid lines) $\alpha \neq 0$ (dashed lines). At point P_1 of Fig. 7: one stable gas (V) phase. The liquid phase (L) is metastable. At point P_2 of Fig. 7: coexistence of the liquid (L) phase and the gas (V) phase of different values of average density. At point P_t of Fig. 7: triple point for coexistence of the liquid phase (L) and the gas (V) phase for different average density with the solid crystalline phase (S).

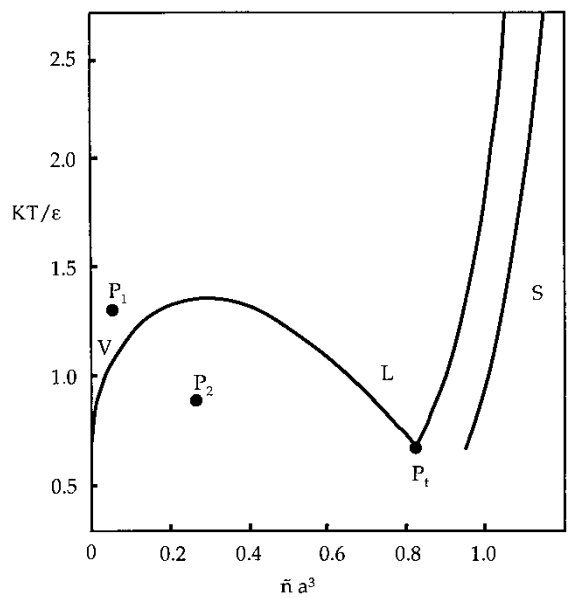

FIGURE 7 The temperature T, density $\tilde{n}$ phase diagram of a Lennard Jones particle of radius a and interaction parameter ε. The points P_1, P_2. P_t are explained in Fig. 6.

diagrams for many different types of systems with resulting scaling. It is a good starting point to test possible model potentials and can predict and explain new phases and empirical laws and even be applied to nanosized aggregates.

In mixtures, new effects occur. For a range of temperature, phase separation can be observed (Fig. 2). The system will then consist of phases of different composition (Guggenheim, 1952). This phenomenon is especially important in polymer systems and the theory to explain why phase separation occurs is an early application of DFT.

3. PHASE SEPARATION IN MIXTURES

3.1. Introduction

Two materials can be combined to obtain synergy of the properties of each individual. Adding a dye to a polymer melt to obtain a colored plastic is an example, but also mixing a polymer in a solvent in order to draw synthetic fibers. For example, cellulose must be diluted in a solvent before spinning of viscose fibers and finding a good, cheap and nonpolluting solvent is still a topical problem. Hopefully a theory could foresee which of the thousands of solvents would be the best candidate and give the reasons why, at least along broad guidelines. Density functional theory is easily extended to mixtures and the very successful Flory Huggins theory of polymer solutions is an example of an early "density functional" theory (Flory, 1953; Hill, 1962). The main effort is to derive a good model for the thermodynamic potential as a function of the density with a minimum of simplifying assumptions. The original papers used a lattice theory to calculate the expression for the free energy or rather the Gibbs potential and to derive the phase diagram in the case of two components based on interaction parameters. Once a model for the interaction is chosen and the thermodynamic potential derived, the method proceeds as before, with minimization in density of the two components, numerical or analytical solution of the resulting equations and plotting of phase diagrams. Different phases are characterized by different values of the number density of the two components.

More recent work relies on a functional integral representation of the partition function (McMullen and Freed, 1990). The advantage of functional integration is found in polymer problems with application to flexible and semi-rigid chains, direct calculation of the chain conformation, simple extension to nonuniform systems and to dynamics (Lifshitz *et al*., 1978). It will be sketched in the following for a concrete application, the calculation of phase separation in a system consisting of flexible polymer chains diluted in a "simple" or nonpolymeric solvent at the temperature T and chemical potential μ (Hong and Noolandi, 1981). The parameters of the polymer are the number of monomer units N_p, the degree of polymerization L_p, the elastic constant of the polymer chain, the interaction between distant monomers V_{pp}. Similarly, the number density N_s ($L_s = 1$) and solvent interaction V_{ss} characterize the solvent. In the mixture, the monomer–solvent interaction V_{sp} is important. The partition function is the phase integral of the relevant Boltzman factors. It is convenient to use a symbolic notation for the polymer chain as a continuous elastic line and the integral in phase space as a functional integral. More on the definition and use of functional integrals can be found in Doi and Edwards (1986).

3.2. Calculation of the Phase Diagram of a Polymer Solution

(1) How to include the chain structure of the polymer?

The partition function contains four terms in V_{ss}, V_{sp} and V_{pp} and in the elastic energy of the polymer chain, which measures the energy required on extension. The "long range" interactions are written with help of the microscopic density of monomers $\hat{n}_p(\boldsymbol{r}) = \sum_{j,m} \delta(\boldsymbol{r} - \boldsymbol{r}_m^j)$ where r_m^j is the position of the monomer m of the jth polymer (the length b of a monomer can be used to scale positions and lengths) and the density

of solvent particles $\hat{n}_s(\boldsymbol{r}) = \sum_l \delta(\boldsymbol{r} - \boldsymbol{r}_l^s)$. The long range interactions donate a term in $\hat{W} = (1/2kT)\Sigma_{\kappa\kappa'} \int d\boldsymbol{r}\, d\boldsymbol{r}'\, \hat{n}_\kappa(\boldsymbol{r}) V_{\kappa\kappa'}(\boldsymbol{r} - \boldsymbol{r}')\hat{n}_{\kappa'}(\boldsymbol{r}')$.

The interaction between nearest neighbor monomers replaces the potential by an effective elastic energy and the resulting distribution of monomers is a Gaussian

$$P_p(\boldsymbol{r}_m^j - \boldsymbol{r}_n^j) = \left[\frac{3}{2\pi b^2 |n-m|}\right]^{3/2} \exp\left[-\frac{3(\boldsymbol{r}_m^j - \boldsymbol{r}_n^j)^2}{2b^2|n-m|}\right]$$

The partition function for the polymer solvent mixture is then

$$Q_{N_\kappa} = \int \prod d\boldsymbol{r}_m^j d\boldsymbol{r}_i^s P_p(\boldsymbol{r}_m^j - \boldsymbol{r}_{m-1}^j) e^{-\hat{W}} \frac{\Lambda_p^{-N_p/L_p} \Lambda_s^{-N_s}}{(N_p/L_p)!\,(N_s)!}$$

where Λ_κ is the contribution of the kinetic energy.

The free energy F is obtained from $e^{-F/kT} = Q_{N_\kappa}$.

(2) How to express the free energy functional?

Mean field theory is used: in the interactions, $\hat{n}_\kappa(\boldsymbol{r})$ is replaced by the average $n_\kappa(\boldsymbol{r})$ and a Boltzmann factor $e^{-\Sigma u_\kappa/kT}$ in the effective "external" potentials u_k is introduced into $Q_{N\kappa}$ to obtain F as a functional of $n_\kappa(\boldsymbol{r})$ and u_κ. The variation of the thermodynamic potential is performed with the supplementary condition of constant particle number, which defines the local chemical potentials μ_k of the monomers and the solvent and thus, the model for Ω in the solution is found.

The functional Ω is obtained by the Legendre transformation

$$\Omega(n_\kappa, u_\kappa) = -F(n_\kappa, u_\kappa) + \int d\boldsymbol{r}\, n_\kappa(\boldsymbol{r})(\mu_\kappa - u_\kappa(\boldsymbol{r}))$$

The minimization of Ω in density and mean field leads to

$$u_\kappa(\boldsymbol{r}) = \sum_{\kappa'} \int d\boldsymbol{r}' V_{\kappa\kappa'}(\boldsymbol{r} - \boldsymbol{r}') n_{\kappa'}(\boldsymbol{r}')$$

$$n_\kappa(\boldsymbol{r}) = -\frac{N_\kappa}{L_\kappa} \frac{\delta \ln Q_\kappa}{\delta u_\kappa}$$

where the partition function of solvent is found to be $Q_s = \int d\boldsymbol{r} e^{-u_s(\boldsymbol{r})/kT}$ and that of the polymer $Q_p = \int d\boldsymbol{r}(\ell) \exp(-\int_0^{L_p} d\ell[u_p(\boldsymbol{r}(\ell)/kT) + (3/2b^2)(d\boldsymbol{r}(\ell)/d\ell)^2])$. Functional integration notation has been introduced to simplify the expression. The average interaction on a monomer or solvent atom is seen to be the average interaction over all other particles, the density of the monomers considers all possible conformations of the chains as given by the elastic line $\boldsymbol{r}(\ell)$, ℓ measures the distance to the origin and replaces the indices.

In the liquid, the densities and mean fields are uniform. It is useful to introduce the concentration or volume fraction of polymer ϕ. In the pure materials, a monomer or a solvent particle occupies a volume v and the density is $1/v$. In the solution of total volume V, the solvent number density is $n_s = N_s/V$, the monomer density is

$n_p = N_p/V$. If the volume occupied by a monomer does not change on dilution, $\phi = vn_p$ and $1 - \phi = vn_s$.

The free energy of mixing $\Delta F = F - \phi F_p/L_p - (1-\phi)F_s$ relative to the bulk materials F_κ (partition function Q_k^0) simplifies to

$$\frac{\Delta Fv}{kTV} = (1-\phi)\ln(1-\phi) + \frac{\phi}{L_p}\ln\phi - \chi\phi(1-\phi) - \frac{\phi}{L_p}\ln\frac{Q_p}{Q_p^0} - (1-\phi)\ln\frac{Q_s}{Q_s^0}$$

The expression originally derived by combinatorial considerations on a lattice in the simple Flory Higgins model is recovered if the change of conformation on dilution is neglected. The mixing behavior is determined by the Flory interaction parameter $\chi = -(1/2kT)(\bar{V}_{ss} + \bar{V}_{pp} - 2\bar{V}_{sp})$ and the nearest neighbor interactions are found to be $\bar{V}_{\kappa\kappa'} = \frac{1}{v}\int d\boldsymbol{r} V_{\kappa\kappa'}(\boldsymbol{r})$.

(3) How to calculate the phase diagram?

The calculation of the phase diagram continues by minimization in ϕ of the "osmotic pressure" $\Delta\Omega = \Delta F - \phi\mu$ to obtain the equilibrium concentration of polymers at a given temperature T for constant "chemical potential" μ. The $\chi(\phi) \sim T^{-1}$ plot is often used (Figs. 8 and 9). As before, various solutions occur. If only one physical solution is found, a uniform atomically dispersed phase occurs at that temperature. Two solutions ϕ and ϕ' signal the appearance of phase separation with coexistence in a biphase of equal osmotic pressure $\Delta\Omega(\phi) = \Delta\Omega(\phi')$ and equal chemical potential μ. If ΔF is plotted as a function of ϕ, it is found that for $\chi < 1/2$, only one solution occurs whereas for $\chi \geq 1/2$ two minima occur. In this case, there is an advantage for unlike particles (a monomer or a solvent atom) to be placed close enough to interact, relative to interaction with near particles of the same species. The phase diagram $\chi^{-1}(\phi)$ shows a large range for which separation occurs. At equilibrium two phases

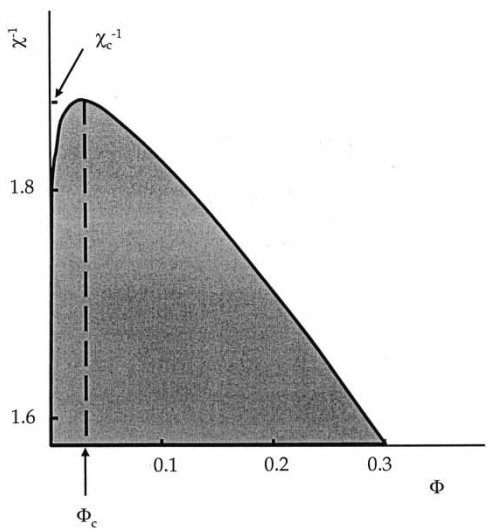

FIGURE 8 The temperature χ^{-1} for a polymer of volume concentration ϕ in a simple solvent. The degree of polymerization of the polymer is 1000. Above the critical point χ_c and concentration ϕ_c only one phase exists. The zone of coexistence is shaded.

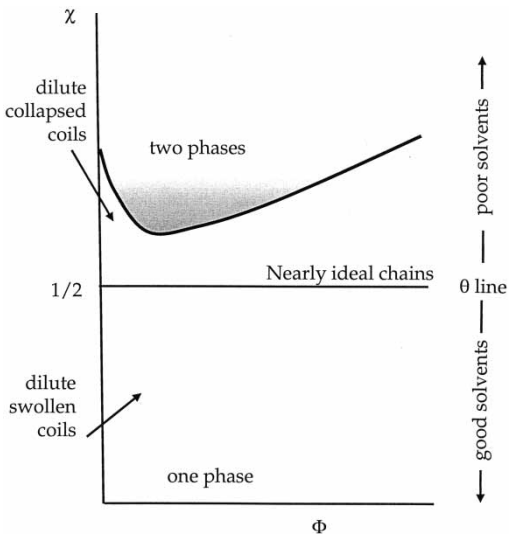

FIGURE 9 Polymer conformation for the phase diagram of Fig. 8.

can be found: usually at room temperature, a solvent phase with few monomers coexists with a polymer phase with little solvent. This is in contrast to the special case of a mixture of two simple liquids with $L_p = 1$. The critical point is found to be a strong function of the degree of polymerization (DP), or number of monomer units in a chain L_p:

$$\phi_c = \frac{1}{1+\sqrt{L_p}}, \qquad \chi_c = \frac{(1+\sqrt{L_p})^2}{2L_p}$$

It shifts from $\phi_c = 1/2$ in simple liquids with $L_p = 1$ to $\phi_c = 0$ for long polymer chains with $L_p \to \infty$. Interaction potentials are usually weak relative to kT and large zones of biphase separation occur in most polymer solutions unless specific interactions (often due to H-bonds) are present. χ values have been measured for many combinations and can be found for example in Flory (1953).

(4) To what systems can the theory be applied?
The extension to a mixture of polymers of degrees of polymerization L_A and L_B is straightforward. It is found that for $L_A = L_B = L$, χ_c is small and $\to O$ as L increases. Miscibility is exceptional and it is better to use systems of very different DP to obtain a uniform solution.

Ternary systems are also easy. Generally, the phase diagrams is given at each temperature in the form of a triangle with each point inside the triangle corresponding to the three concentrations. The limits of the biphasic zones are then given at each T. An example is shown in Fig. 10.

In the simplest theory χ varies as $1/T$ and the effective potentials $V_{\kappa\kappa'}$ do not vary with temperature. It can happen though that the potential is temperature or concentration dependent and more complex forms of χ are needed to fit to experiment. For example: H-bonds are often formed in cellulose derivatives in solution and break at high temperature. A lower critical solution temperature is found with strong phase

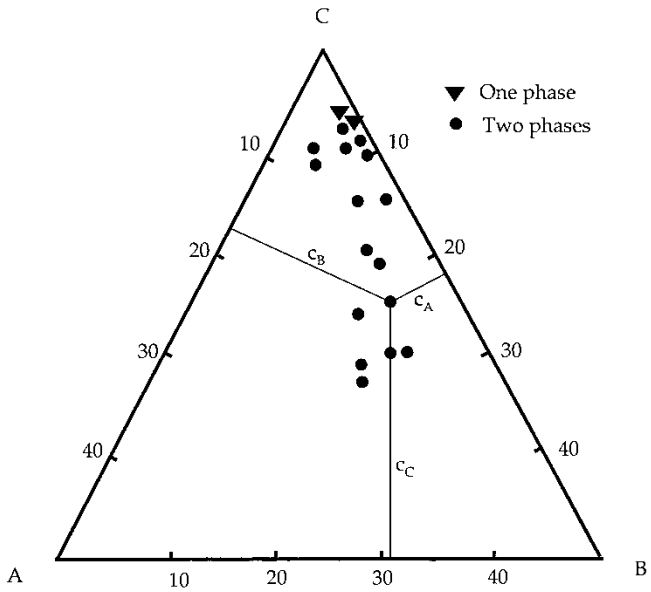

FIGURE 10 Phase diagram for a ternary mixture ABC. The concentrations c_A, c_B, c_C are given by the lengths of the perpendicular lines.

separation at high temperatures which in some cases, even leads to gel formation. The simple mean field DFT cannot be used except as a rough estimate if strong local effects are present such as specific chemical bonding. It can also not be used to follow the change of chain conformation in solvent.

3.3. Polymer Conformations

The single chain distribution function can be calculated (in principal) in the presence of the excluded volume potential defined as the effective interaction between monomers. The chain conformation is measured by the end-to-end distribution function for any initial position r_0 of the chain origin:

$$G(\boldsymbol{r}, L) = \int d\boldsymbol{r}_0 d\boldsymbol{r}(\ell) \exp\left(- \int d\ell \left[\frac{u_p(\boldsymbol{r}(\ell))}{kT} + \frac{3}{2b^2} \left(\frac{d\boldsymbol{r}(\ell)}{d\ell} \right)^2 \right] \right) \delta(\boldsymbol{r} - \boldsymbol{r}(L)) \delta(\boldsymbol{r}_0 - \boldsymbol{r}(0))$$

The distribution can be shown to satisfy a modified diffusion equation within the effective potential

$$\frac{\partial G(\boldsymbol{r}, L)}{\partial L} = \frac{b^2}{6} \Delta G(\boldsymbol{r}, L) - \frac{u_p}{kT} G(\boldsymbol{r}, L)$$

The monomer density can be expressed as

$$n_p(\boldsymbol{r}) = \frac{N_p}{L_p Q_p} \int_0^{Lp} d\ell G(\boldsymbol{r}, \ell) G(\boldsymbol{r}, L_p - \ell)$$

From these two equations and the definition given previously of the concentration dependent mean field u_p between monomers, the single chain distribution function can be calculated self-consistently. The existence of correlation between monomer positions and screening with adaptation of the polymer chain to minimize the interaction with the surrounding environment has prompted the use of more powerful methods but the essential features turn out to be the same (Yamakawa, 1971; de Gennes, 1979; Doi and Edwards, 1986).

In the classical Flory theory, the average change in the extension of the polymer on dilution in a solvent is estimated from assumptions on the monomer concentration and from the DFT expression for the free energy of mixing derived above. In dilute solution the effective repulsive interaction is found by expanding the Flory free energy in the volume concentration $c = \phi/b^3$. The term in c^2 defines the mean field value of the "excluded volume" interaction between two monomers $v = b^3\ (1 - 2\chi)$.

In a dilute good solvent, $v > 0$. An average chain of L_p monomers will fill a sphere of radius R and the effective concentration inside the polymer coil which determines the mean field is $c = L_p/R^3$. The distribution of the final monomer is $G(R,\ L_p) \propto \exp(-H(R))$ with $H(R) = (3R^2/2L_pb^2) + cv$. By minimization of H in R, the relation $R^5 = vb^2L_p^3$ is found for the most probable value of end-to-end distance R.

In a bad solvent, $v < 0$ and each polymer chain is contained inside a sphere of radius R and concentration ϕ'' floating in a solvent of concentration ϕ'. Then $\phi'' = L_pb^3/R^3$ and from the calculation of the phase diagram $\phi'' = -3v/2b^3$. The chain extension varies as $L_p^{1/3}$.

At the θ point the effective interaction vanishes and the repulsive interactions which cause the polymer conformation to shrink are balanced by the entropy or elastic terms. The conformation is ideal and R follows a law $L_p^{1/2}$ as in the ideal Gaussian distribution. (Fig. 9). These results have been confirmed by neutron scattering and more extensive theories.

4. LIQUID CRYSTALS

4.1. Introduction

Liquid crystal display devices (LCD) play a very important role by providing a low energy, mobile person–machine interface as flat planel displays continue to improve and to lower in price. The principle of a liquid crystal display is sketched in Fig. 11 and is based on the coupling of the optical properties of the liquid crystal (LC) material and an electric field. LC molecules tend to align due to their chemical structure and the molecular orientation is sensitive to an applied electric field. The LC is confined in a cell between glass plates coated with a transparent conducting film. Crossed polarizers are placed at the two ends. The glass substrate surface is treated to force the molecules to orient parallel to a fixed direction causing a twist along the axis of the cell. The polarization of incoming light is twisted due to the electrical dipoles in the molecules and is transmitted. When the electric field is applied, the electrical dipoles cause the LC molecules to align parallel to the field, the polarization of the incoming light remains unchanged and no light can escape from the cell. Each pixel in a LCD can be addressed by the applied field to produce a light or dark image following an information signal.

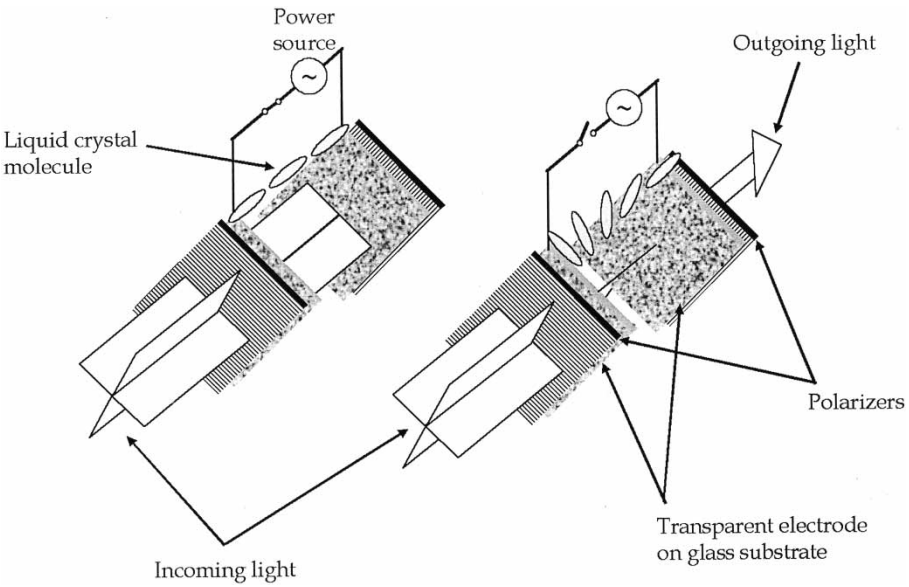

FIGURE 11 A twisted nematic display.

The fundamental problems involved in a LCD are manifold and have been modeled with DFT as will be discussed in the following.

Some of the questions that have been investigated are

– Why do the LC molecules have a tendency to align?
– How is the alignment affected by the electric field?
– How does the substrate align the LC molecules and what methods can be used to improve the anchoring?
– How is the light affected by the molecular orientation?

Answering these questions, even in an approximate way, can serve as a guideline in the choice of liquid crystal material and point to the directions for synthesis of new materials with specific properties. The first two were investigated with a DFT theory and will be discussed. The third enters into problems of the interface and will be treated in the next chapter. Light scattering and the relation to the average orientation can be found for example in Stephen and Straley (1974).

Historically (in the mid 1800s), the liquid crystal phase was first thought to be a two-phase coexistence region in the phase diagram due to the presence of an impurity. Biological materials were investigated in polalized light and, in contrast to most liquids, were shown to produce changes in light polarization. In 1888, Reinitzer found an organic material with an intermediate cloudy liquid phase, and examined in the microscope Lehman concluded the existence of a new uniform phase that could effect polarized light. Materials of linear molecules were then synthesized and the first commercial LCD devices appeared in 1960. Fig. 11 shows the most common display method of the twisted nematic. LCs can be natural, biological materials (DNA, cellulose, collagen, tobacco mosaic virus) or synthetic (PAA, MBBA). The molecular structure is rigid, due for example to helical conformation or to benzene rings. The electrical polarizability is large.

4.2. Maier Saupe Theory

The theoretical model in its simplest form assumes linear molecules characterized by position $\boldsymbol{r}$ and orientation $\boldsymbol{w}$ of the molecular axis (Stephen and Straley 1974; Priestley *et al.*, 1975). The average direction of orientation is called the director and is usually chosen as the z-axis. The probability $n(r, w)$ to find a molecule at position $\boldsymbol{r}$ with orientation $\boldsymbol{w}$ can be assumed to decouple and $n(r, w) = n(r)f(w)$. The number density $n(r)$ is uniform, and $f(w)$ is normalized to unity.

The free energy model is written as an expansion relative to the isotropic phase of random orientation:

$$F(V, T) = kT \int d\boldsymbol{w} f(\boldsymbol{w})(\ln f(\boldsymbol{w}) - 1) + 1/2 \int d\boldsymbol{w} d\boldsymbol{w}' f(\boldsymbol{w}) V(\boldsymbol{w}, \boldsymbol{w}') f(\boldsymbol{w}')$$

The first term is the entropy of the ideal system and the second the interaction, which depends on the relative orientation of the two particles. In a first step, the interaction is not described in more detail. It can have many origins: steric repulsion (match stick effect), Van der Waals, Coulomb. Due to top and bottom symmetry of the molecules, an expansion in spherical harmonics is used:

$$V(\boldsymbol{w}, \boldsymbol{w}') = -AP_2(\boldsymbol{w})P_2(\boldsymbol{w}') \quad \text{with } P_2(\boldsymbol{w}) = 1/2(3\cos^2\theta - 1).$$

θ is the angle of the molecular axis and the z-axis. The position averaged interaction parameter is $A > 0$. The calculation proceeds on variation of the free energy with respect to the function f.

The solution is a mean field expression: $f(\boldsymbol{w}) = c \exp[-\int d\boldsymbol{w}' f(\boldsymbol{w}') V(\boldsymbol{w}, \boldsymbol{w}')/kT]$ with $(1/c) = \int d\boldsymbol{w} \exp[-\int d\boldsymbol{w}' f(\boldsymbol{w}') V(\boldsymbol{w}, \boldsymbol{w}')/kT]$

The order parameter $S = \int d\boldsymbol{w} f(\boldsymbol{w}) P_2(\boldsymbol{w})$ is introduced to describe average orientation and varies between 0 and 1. It can be calculated from the self-consistent equation for $f(\boldsymbol{w})$.

$$S = c \int d\boldsymbol{w} P_2(\boldsymbol{w}) \exp(ASP_2(\boldsymbol{w})/kT)$$

The mean field $AP_2(\boldsymbol{w})S$ appears and measures the interaction of all particles on the particle with orientation $\boldsymbol{w}$. Solution of the equation is done numerically or graphically. Minimization of the functional F with respect to f is equivalent to minimization with respect to the order parameter S. Introducing f into F, the function $F(S)$ can be plotted for different temperatures. At high temperature $F(S)$ has one minimum at $S = 0$ which defines the isotropic phase. As the temperature is lowered a second minimum appears at $S > 0$ (3 possible solutions). At the transition $T = T_c$, $F(S_c) = F(0)$ and at lower temperatures the second minimum is displaced toward $S < 0$. The result for $S(T)$ is given in Fig. 12. The transition is first order with $kT_c = 0.22\,A$ and $S_c = 0.43$. The similarity to the previous calculation is evident: the discussion on the average density is replaced by the orientational order parameter S. Most order–disorder phase transitions can be formulated using this method requiring only a free energy expression and a relevant order parameter.

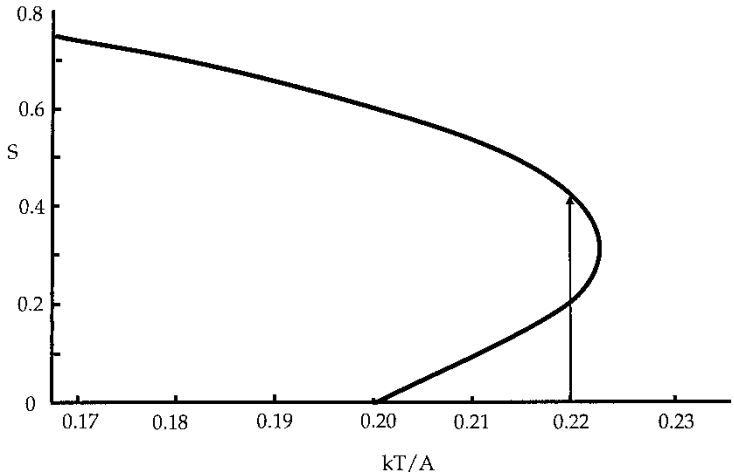

FIGURE 12 The orientational order parameter S as a function of temperature (measured in units of interaction parameter A). The transition from the nematic to isotropic phase is shown by the arrow.

Other LC phases such as cholesterics or smectics have also been investigated with variations of the DFT and proper adaptation of the potential (Fig. 3).

Mixtures of liquid crystals, of liquid crystals with polymers and of liquid crystal polymers (Ronca and ten Bosch, 1991) are of industrial importance and allow selective variation of properties. The phase diagrams in the mixtures can be calculated by adapting Section 3 to include orientation dependence in the pair interaction between molecules and in the density distribution. Extensions beyond mean field theory and for strong hard core effects are discussed in Vroege and Lekkerkerker (1991).

4.3. Nonuniform Phases

The director in many cases is not uniform in the sample (Stephen and Straley, 1974). Even in equilibrium the direction of preferred orientation can vary from place to place or can be forced to vary by the action of external forces and boundary conditions. Nonuniform metastable configurations which do not relax rapidly are caused in the preparation of the sample or by surface boundaries. Discontinuities (or singular defects) in the director orientation occur at certain points and form characteristic patterns when viewed in a microscope.

The response of the liquid crystal to changes of molecular orientation on a large scale relative to molecular distance is described by continuum orientational elastic energy for director deformation (Lubensky, 1970). By symmetry considerations only 3 basic operations are possible: splay, twist and bend, each of which is measured by the corresponding strain and introduces the Frank elastic constants K_s, K_t, K_b. The resulting free energy density relative to state of uniform orientation is

$$F(\boldsymbol{n}(r)) = (1/2)K_s(\nabla \cdot \boldsymbol{n})^2 + (1/2)K_t(\boldsymbol{n} \cdot \operatorname{rot} \boldsymbol{n})^2 + (1/2)K_b(\boldsymbol{n} \cdot \nabla \boldsymbol{n})^2$$

Minimization of the free energy functional leads to a differential equation for the vector components $n_i(r)$, $i = x, y, z$ of the director $\boldsymbol{n}$ which must be solved in the relevant geometry. Electric and magnetic fields are simple to include by adding the electric or magnetic energy. For example, in the presence of an electric field $\boldsymbol{E}$, the additional

term in the energy density of the system is $-(\varepsilon_0 \boldsymbol{E}^2/2) - (\varepsilon_a(\boldsymbol{En})^2/2)$. The functions ε_0 and ε_a are the anisotropic dielectric constants of the linear molecule with a different electrical response // or $\perp$ to the molecular axis. In a typical problem of the twisted nematic there is a conflict between the electric field and fixed surface anchoring and, to orient the liquid crystal molecules parallel to the field, a critical electric field is required.

Recent work in this field has considered liquid crystals dispersed in a polymer matrix (PDLC or polymer dispersed liquid crystals), elastomers (with coupling to elasticity of rubber matrix) and suspensions. In these materials the effect of the surface becomes important and this will be discussed in the following.

5. THE INTERFACE

5.1. Structure and Properties of the Interface

A surface or interface is a contact between different materials or phases (a vapor–liquid surface, the interface between water and oil, a membrane). The contact can be stationary with no variation in time as will be discussed here, or dynamical (a droplet spreads, a crystal layer grows, droplets condense on a surface) as discussed in Section 6. The morphology can be changed by a variation of temperature (drops can evaporate), by application of a field (paint can be spread) and the industrial applications are numerous: paint, lubricants, soaps, catalysts, nanomaterials, composites. A review of surface science experimental methods and industrial applications is given in Somorjai (1998).

In an interface, the properties of the material are different (Isrealachvili, 1992). The particles in the interface have a different environment, for example less or different nearest neighbors or a larger nearest neighbor distance. To study adsorption on a surface or on a polymer, the lattice model discussed for AB mixtures was used to derive the model free energy using $A =$ particle adsorbed on a site, $B =$ empty site (Langmuir model). Recent work in surface problems applies DFT even to thin films. At a surface, the average density (or other order parameter) is a function of position. For example in wetting, a liquid film can be found between the solid and vapor phase or in a polymer solution, the surface concentration can vary. A new phase can appear first at the surface and a surface phase transition is observed.

At the interface, a phase is characterized by the profile of density or the concentration or other relevant order parameter as a function of position. Sometimes two parameters are needed. When a liquid film wets the crystal, both the average density and the crystal structure will vary at the surface. In a nematic–isotropic interface, the average density and the average orientation depend on position. A certain energy (surface or interfacial energy) γ_{11} is necessary to form a surface. The stronger the interaction, as measured for example by the boiling point of the pure material, the larger the energy of cohesion and therefore the surface energy. The interfacial energy between 1 and 2 requires the energy of adhesion W_{11} and W_{22} to separate the two components and create both the 11 and the 22 surface, lowered by the energy of cohesion W_{12} when the 1–2 contacts are formed. Therefore, $\gamma_{12} = (W_{11} + W_{22})/2 - W_{12}$. The form of the surface can be more complicated than a spherical top or the meniscus of a liquid in a contact with the solid surface. On a curved surface the capillary forces cause a normal pressure, the capillary pressure $p = 2\gamma/\rho$, ρ being the radius of

curvature. Surfaces of constant capillary pressure can have complex forms observed for example in soap bubbles, blood cells or chiral membranes (wet paper).

Contact between two materials in the presence of a third leads to wetting phenomena. The contact angle θ is measured. The interfacial tension is the force parallel to the surface of magnitude of the interfacial energy and the Young equation follows from an equilibrium of forces at the contact between the three phases; $\gamma_{13} = \gamma_{12} + \gamma_{23} \cos \theta$. The contact angle minimizes the total surface energy and can vary from $\theta = o$ (complete wetting, for example water–glass) to $\theta = \pi$ (nonwetting, for example water–surfactant–oil). The wetting angle depends on temperature and perfect wetting can occur as the temperature is raised above the wetting temperature. The research in this field is very active and has been addressed by DFT, as well as by numerical simulation methods. The question is extremely important in industry and plays a role in phenomena of adhesion such as in glues and in the production of the heterogeneous materials formed of films, layers, inclusions or coated surfaces. The contact angle is macroscopic but on a molecular level the surface is not sharp but diffuse. For example, in a photographic film, many surface contacts occur (Fig. 13). Some of the questions which must be solved empirically or by testing or through theoretical considerations are:

– choice of materials to obtain the required properties for example elasticity
– stability of the contact with time, temperature
– necessity of coating to enhance adhesion
– effects of geometry, size

These phenomena can be described with DFT, and the results of the theory can assist in predicting behavior under use.

5.2. Square Gradient Approximation

A more precise calculation of wetting phenomena and of interfacial properties in general is based on DFT with position dependent density profiles (Widom, 1991; Evans,

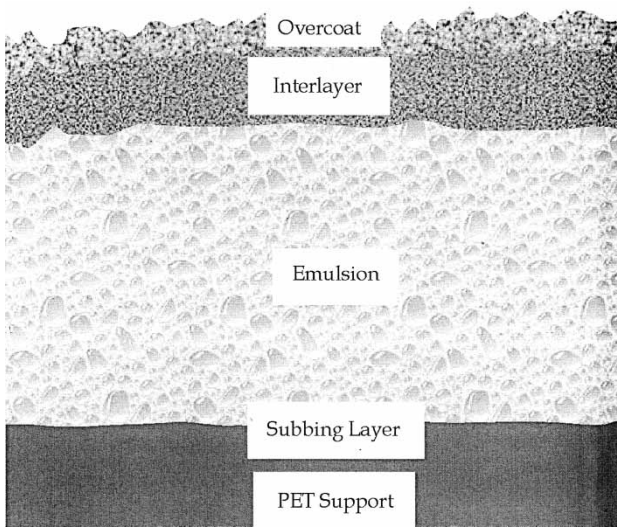

FIGURE 13 Photographic film as a composite material.

1979). The calculation proceeds as given by Steps (1) to (9) of Section 2. The grand potential is $\Omega(T, V, \mu(n)) = F(T, V, \mu(n)) - \mu N(T, V, \mu(n))$. The expansion of Ω with respect to a reference system of density n_0 is found as before from $F = F_{id} + F_{ex}$. The variation of Ω yields the equilibrium profile with $\delta\Omega/\delta n\ (T,\ V,\ \mu(n)) = 0$ or

$$\frac{\mu}{kT} = \ln n(\boldsymbol{r})\Lambda - c^{(1)}(\boldsymbol{r}, n_0) - \int d\boldsymbol{r}'(n(\boldsymbol{r}') - n_0))c^{(2)}(\boldsymbol{r} - \boldsymbol{r}', n_0) + \cdots$$

This nonlinear integral equation is simplified for slow variation of the profile with respect to a well-chosen reference system. A Taylor expansion for the density is introduced into the integral. Due to spatial symmetry the linear terms vanish, only the square gradient terms (SGA) are retained and the equation for the profile becomes: $\mu = \mu(r) = \mu(n(\boldsymbol{r})) - \kappa\nabla^2 n(\boldsymbol{r})kT$ where the volume contribution is

$$\frac{\mu(n(\boldsymbol{r}))}{kT} = \ln n(\boldsymbol{r})\Lambda - c^{(1)}(\boldsymbol{r}, n_0) - \alpha_0(n(\boldsymbol{r}) - n_0) + \cdots$$

$$\alpha_0 = \int d\boldsymbol{r}\, c^{(2)}(\boldsymbol{r}, n_0)$$

α_0 is the contribution due to the interaction of the particles or the first moment of $c^{(2)}(r,\ n_0)$ and the term which measures deformation of the surface is the second moment of $c^{(2)}(r,\ n_0)$:

$$\kappa = \frac{1}{2}\int d\boldsymbol{r}\, \boldsymbol{r}^2 c^{(2)}(\boldsymbol{r}, n_0).$$

The nonlinear differential equation for $n(r)$ is solved using physically intuitive boundary conditions. Far from the interface, the system is separated into the two bulk coexisting phases of density n_1 or n_0 given by the phase diagram. The conditions of thermodynamic equilibrium require constant chemical potential and pressure.

In a linear approximation, the local chemical potential $\mu(n(r))$ is expanded to first order in $n(r) - n_0$ and the boundary condition $\mu = \mu(n(\infty)) = \mu(n_0)$ is used. The equation for $n(r)$ is a simple self-consistent equation. $n(\boldsymbol{r}) - n_0 = \xi^2\nabla^2 n(\boldsymbol{r})$. The decay length is $\xi^{-2} = (n_0^{-1} - \alpha_0)/\kappa$. For the planar interface of area A in the x direction, the solution is: $n(x) = n_0 + (n_1 - n_0)\exp(-x/\xi)$.

The surface energy is found from $\gamma = (\partial\Omega/\partial A)_{T,V,\mu}$. For the planar interface, using the boundary condition of vanishing density gradient far from the zone of contact

$$\gamma = \int dx\left[f(n(x)) - \mu n(x) + \frac{\kappa}{2}\left(\frac{\partial n(x)}{\partial x}\right)^2 kT\right].$$

Here $f - \mu n$ is the volume energy contribution for formation of the surface with $\mu(n(x)) = \delta\int dx f(n(x))/\delta n(x)$. For example in the linear approximation: $\gamma/kT = \kappa(n_1 - n_0)^2/2\xi$. The equilibrium profile is obtained for the minimum surface energy, allowing an alternate method of solution.

In a different approach using thermodynamic perturbation theory, the free energy is expanded in a hard sphere reference system. The potential between particles is approximated by the repulsive hard sphere interaction and an attractive potential $\varphi(r)$. The expression for the free energy of the hard sphere system is known. The grand potential can then be minimized with respect to the parameters to obtain the equilibrium profile and the resulting surface energy.

Much effort has gone into an accurate definition of the free energy functional and discussion of possible phenomena in model systems. Most of the work has been done for the one-dimensional interface. Spherical droplet geometry is still relatively unexplored, the stationary droplet shape being one exception. The method is general insofar as the local chemical potential can always be given as a volume term and a surface term. If the density gradients are small in the range of the potential, the square gradient approximation can be used. The equilibrium profile also follows from variation of the functional $\gamma(n(r))$. The many spurious solutions must be eliminated with help of physically reasonable boundary conditions.

5.3. Wetting

The question is to find under what conditions complete wetting occurs for a contact between three materials or phases denoted 1, 2, 3 (Dietrich, 1991; Tarazona and Evans, 1983).

In the simplest approach, wetting is said to occur when a film of 2 of thickness h forms between 1 and 3. An effective surface potential per unit area is derived as a function of h which plays the role of an order parameter. The energy to create a 123 surface of width h is

$$\Delta(h) = \gamma_{12} + \gamma_{23} + (e_2 - e_3)h + be^{-h/\xi} + \sum \frac{a_n}{h^n}$$

The first two terms measure the surface energies at the 1–2 and 2–3 contacts. The third term is a volume energy: $e_2 - e_3$, a measure of the gain when the 2 phase is inserted in place of 3. The origin of the fourth term is the finite decay length of the density profile leading to an effective interaction between 1 and 3 through the layer of 2 due to short range forces. The final term considers long range forces between 1 and 3 through 2. The term in a_2, known as the Hamaker constant, is the most important and is caused by the induced dipolar interaction between surface layers.

In the simplest case, the short range forces dominate. The thermodynamic potential is minimized with respect to h and for $b > 0$. At the wetting temperature, the phases 1, 2 and 3 have equal values of grand potential which shows three minima. To study the temperature dependence of the thickness, the volume terms are expanded $e_2 - e_3 = -H(T - T_w)$ near the wetting temperature $T = T_w$ and the thickness $h \approx \ln(T_w - T) \to \infty$ (Fig. 14). In a similar way, if short range forces are absent and the Hamaker force dominates and $a_2 < 0$ then $h \approx (T_w - T)^{-1/3}$. A plot of film thickness as a function of temperature can indicate the type of surface forces which dominate (Chen *et al.*, 1991). Sometimes a transition from one behavior to another occurs as long range forces become screened out in sufficiently thick films.

Wetting is easily discussed with the phenomenological potential. The thickness of a wetting film depends on a balance between surface and volume energy. If a volume energy is lost by a replacement of phase 3 by 2, the system gains by increasing

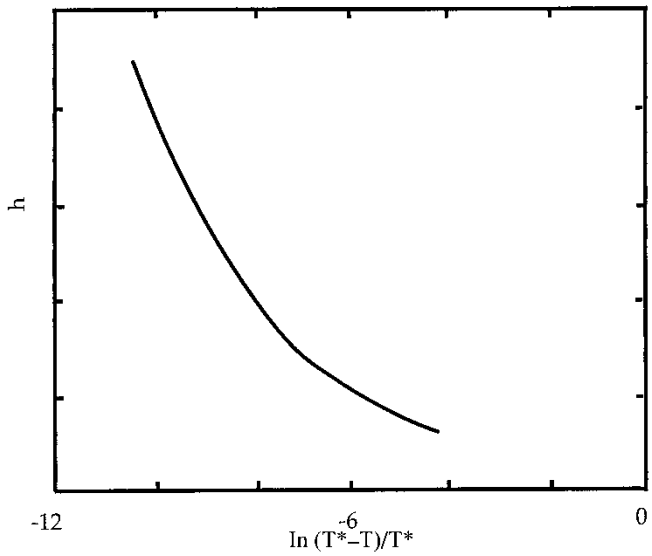

FIGURE 14 Width h of the wetting layer as a function of temperature T (Chen et al., 1991).

the thickness sufficiently to balance the surface repulsive positive energy. If the volume energy difference is negative, the system cannot gain enough energy by a finite layer size, the thickness must be macroscopic. More complex cases are discussed in Dietrich (1991). Experiments are in agreement with some of these predictions but research in this field is still active.

A test of the theory is found in surface phase transitions for which the new phase appears at the surface at a temperature below the bulk transition (Löwen, 1994). "Wetting" of the old phase by the new occurs, observed for water on ice by Faraday in 1842 and in melting of rare gases and metals. The phenomenological theory has been successfully applied to the surface transition in nanoclusters at the melting point.

5.4. Extensions to Crystals, Liquid Crystals, Polymers

Extensions have been made to a *crystalline surface* covered by the liquid at the triple point (Oxtoby, 1991). In the phase diagram given in Fig. 7, the triple point can be approached along the solid–gas coexistence line. In the crystal, the density is a periodic function as was shown previously. The crystallinity is described by the vectors of the crystal structure and by the density distribution on each crystal site. Within the (crystal–gas) interface, these quantities will vary as well as the average density. In a DFT approach, the first step requires a calculation of the phase diagram. The coexisting phases are found for a given pressure and temperature by minimization of the functional Ω. The interfacial properties of the coexisting phases can than be calculated by considering the density in the square gradient expansion which contains two parts; the variation of the average density $\tilde{n}(x)$ in the interface and of the width of the density distribution around crystal sites $\alpha(x)$. The periodicity of the crystal is assumed to remain unchanged in the interface, a more detailed calculation would consider small shifts in the equilibrium sites. The profiles follow on solution of the two coupled differential equations for $\tilde{n}(x)$ and for $\alpha(x)$. The boundary conditions are the

values of the parameters in the pure solid or gas phases. A typical profile (for example in a metal) shows a continuous change of the average density over 6–20 atomic layers. The atoms slowly lose the localization on crystal sites; the size of the interface depends on temperature. At the triple point, the thickness of the interface $\rightarrow \infty$ with perfect wetting of the crystal by the liquid phase and surface melting. The surface energy can also be calculated and is of course dependent on the facet or crystal structure of the surface.

Liquid crystal interfaces have also been investigated in DFT. In the expression for the free energy the distribution function $f(r, w)$ depends on the position as well as the orientation of the molecules. Using the SGA, a position dependent orientation $S(\boldsymbol{r}) = \int d\mathbf{w} f(\boldsymbol{r}, \boldsymbol{w}) P_2(\boldsymbol{w})$ and density $n(\boldsymbol{r}) = \int d\boldsymbol{w} f(\boldsymbol{r}, \boldsymbol{w})$ appear. The free energy functional is minimized with respect to the profiles $S(r)$ and $n(r)$. In the simplest problem the density change is neglected and only the order parameter profile contributes to the surface properties, but more general cases have been explored. In order to calculate the nematic–isotropic interface a Lennard Jones or other model potential is inserted in the equation for the equilibrium chemical potential. Again, to fix the boundary values at coexistence, the first step requires a model for the bulk free energy functional of average density and orientation and calculation of the phase diagram.

Wetting phenomena and surface phase transitions follow in these systems with new effects due to orientational order at the surface (Telo da Gama, 1984; Sullivan and Telo da Gama, 1986). An important application of the theory is found in surfactant interfaces and micelles, with strong orientational order in the boundary layers. Even in systems which do not have a sufficiently strong intermolecular interaction to form a liquid crystal phase, orientational order can occur in a narrow layer close to an active surface (Fig. 15).

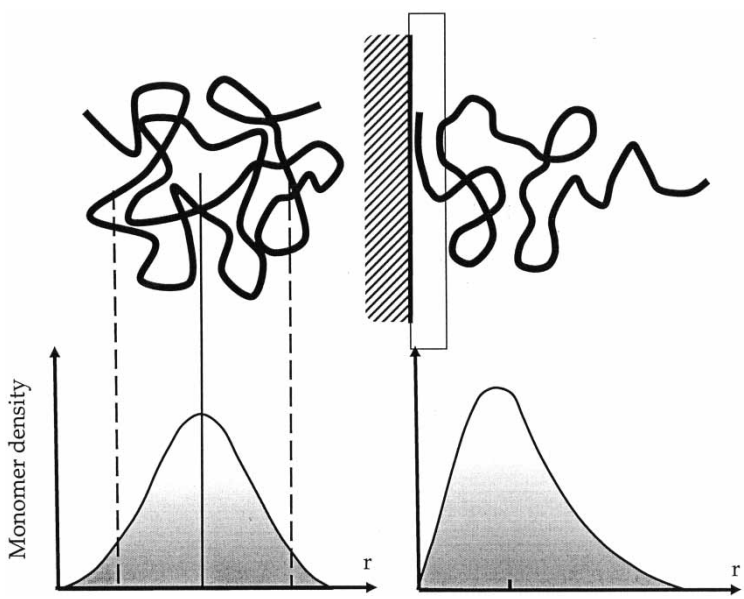

FIGURE 15 Effect of a wall on a polymer conformation.

In liquid crystal devices, the director orientation can be fixed at the surface by appropriate sample preparation (anchoring) and interaction with the substrate or, for short range effects, a boundary condition on the director must be considered. In polymer dispersed liquid crystals, globules of liquid crystals are formed inside a polymer matrix. The average orientation can be strongly nonuniform due to the globular geometry. The curvature elastic energy will be minimized in the presence of the complex boundary conditions and often defects in the director field cannot be avoided (Jeróme, 1991).

For the *polymer interface*, in the simplest mean field approach, the average monomer density or concentration is calculated as in a simple atomic liquid. The sample parameters are fixed in order to adapt to the dense liquid structure and reproduce the phase diagram.

Polymers are distinguished by interactions inside the chain which, especially in solution, will be different in the interface as compared to the bulk. The calculation of the interface must consider the effect on the molecular conformation.

For coexistence between a phase separated system of polymer in a solvent, the elastic chain model has been used to describe the variation of the polymer conformation. (Hong and Noolandi, 1981). The "diffusion" equation for the single chain distribution G is solved in the position dependent, excluded volume mean field which depends on the local monomer concentration, determined self-consistently from G. For a planar interface, the surface energy has been derived in the elastic chain model in the SGA and consists of a "bulk" contribution due to the change of the local chemical potential from the bulk value and a "surface" contribution $1/2\kappa(d\Phi/dx)^2$ from the concentration profile $\Phi(x)$. The constant κ is the second moment of the interaction on a monomer of the polymer chain. In solution, $\kappa \approx b^2\chi$ where χ is the Flory parameter and b the monomer size. The intrinsic parameters of interest are the degree of polymerization L and the Flory interaction. As a rule the width of the interface is largest for small χ and L, and the value of the interfacial energy is smallest. Temperature and concentration dependence can be studied, and the agreement with experiment is satisfactory as with the empirical laws $\gamma = \gamma_0 + cT$ and $\gamma_\infty - c'/L$ (c, c' are constants in T or L).

The conformation of the polymer is strongly affected by the contact surfaces. Non-Gaussian distribution is found for chemisorption and physisorption as well as crowding at high concentration and in small samples. In principle these effects can be included in a DFT as well as certain details of the molecular structure: the asymmetric chain ends of self-organized membranes, chirality, rigidity, orientational interactions.

6. DYNAMICS

6.1. Time dependent Density Functional Theory

Many problems in materials science are concerned with time dependent phenomena. A drop of paint on a wetting surface is not in a stationary state and will spread with time, changing shape and profile (de Gennes, 1985). Industrial materials are affected by phase transitions which occur during production: phase separation in mixtures, crystallization inside the sample, condensation at the surface. As an example in materials processing, thin metal films can be prepared by vacuum deposition. A flux of metal atoms in vacuum is allowed to deposit on a substrate forming aggregates, and/or films as condensation from the vapor accrues. The size, morphology and properties

of the material are sensitive functions of external conditions such as temperature of the substrate or the characteristics of the metal–substrate pair.

Much work, theoretical as well as experimental, has been expended on achieving a better comprehension of the processes involved. A type of time dependent density functional theory would be well adapted to study mesocopic dynamical systems. The question is how to extend the well established theory of equilibrium phases.

6.2. Field Theory

A phenomenological approach has been used extensively (Hohenberg and Halperin, 1977, Gunton *et al.*, 1983). Model equations are proposed to describe the kinetics of the density $n(r, t)$ in space and time, introducing phenomenological parameters. In the following Γ is the constant which relates the flux and the force. F is a (free energy) thermodynamic functional of $n(r, t)$ (often simply a Landau expansion or power series in n) and derivatives of $n(r, t)$ which are chosen to give the correct equilibrium and stationary behaviour. Some examples are:

- The Landau Ginzburg equation is also known as Model A: $(\partial n/\partial t) = -\Gamma(\delta F/\delta n)$. The driving force is the local chemical potential, the equilibrium phase is found from $\delta F/\delta n = 0$.
- In Model B, also known as the Cahn Hilliard equation, the driving force is the gradient of the local chemical potential: $(\partial n/\partial t) = \Gamma\Delta(\delta F/\delta n)$.

In both cases, the equilibrium phase is flux free with constant chemical potential and pressure.

As in equilibrium systems, the density distribution can depend on other variables besides position: orientation of the molecular axis, localization of density on a crystal site, width of a surface layer. In the effective mean field treatment of DFT, these local quantities are replaced by global averages, the order parameters. An order parameter is the dynamic average of a space and time dependent property of the particles. The kinetic equation for the density distribution can be transformed into kinetic equations for the order parameters. For example, in a liquid crystal, the Landau Ginzburg equation for the order parameter $S(r, t)$ is derived from the equation for the distribution: $n(r, w, t)$ using model A. Model A is considered valid if no conservation law is involved for the order parameter, as for example the orientational order parameter in a liquid crystal. In model B, a conservation law is implied.

- Sometimes more than one parameter is needed. For example, in crystals, the crystallinity or in liquid crystals, the average orientation as well as the average density are used to describe the kinetics. A system of equations results, such as in model C which is a combination of models A and B for one nonconserved and one conserved order parameter.
- Often hydrodynamic flow occurs spontaneously or is applied. Crystallization in a shear flow is a well-known example. Flow effects are then important and have been considered in model H.

6.3. The Atomistic Approach of Kinetic Theory

Phase field models have been used extensively and with some success to study dynamic properties but without further justification besides the interest and availability of a

model for the functional F. Attempts have been made to derive the field equations from a microscopic theory such as the *master equation* for the probability distribution of the system or the *Liouville equation* in phase space (Langer, 1971; Montroll and Lebowitz, 1987). The global probability $P(r_1, r_2, r_3,\ldots,t)$ to find particles simultaneously at given positions $\boldsymbol{r}_i$ in space at a given time, eventually with a given velocity $\boldsymbol{v}_i$, orientation or other independent characteristic, is required in order to perform a dynamical system average. For example, to calculate the average number $n(\boldsymbol{r}, t)$ of particles at position $\boldsymbol{r}$ at a time t:

$$n(\boldsymbol{r}, t) = \left\langle \sum_i \delta(\boldsymbol{r} - \boldsymbol{r}_i) \right\rangle = \int d\boldsymbol{r}_1 d\boldsymbol{r}_2 \cdots P(\boldsymbol{r}_1, \boldsymbol{r}_2 \cdots t) \sum_i \delta(r - \boldsymbol{r}_i)$$

or the local velocity given by the flux: $\boldsymbol{j}(\boldsymbol{r}, t) = \left\langle \sum_i \boldsymbol{v}_i \delta(\boldsymbol{r} - \boldsymbol{r}_i) \right\rangle$

The problem is greatly simplified for independent particles for which $P(r_1, r_2, r_3,\ldots,t) = \Pi\ P(r_1 t)P(r_2 t)P(r_3 t)$. But as a rule, particle movement is not independent. Various correlation functions are accessible from experiment which reveal details of the average motion of the particles of the system:

- the pair correlation function: $g(\boldsymbol{r} - \boldsymbol{r}', t) = \left\langle \sum_{i,k} \delta(\boldsymbol{r} - \boldsymbol{r}_i)\delta(\boldsymbol{r}' - \boldsymbol{r}_k) \right\rangle$ and its Fourier transformation, the dynamic structure factor $S(q, \omega)$
- the mean square displacement, used to define the diffusion constant
- the velocity correlation, used to define the friction constant

Nonequilibrium thermodynamics applies thermodynamic considerations to irreversible processes and provides a general framework for a description of processes not too far from equilibrium (de Groot and Mazur, 1962; Chandrasekhar, 1943). State parameters are treated as field variables and fulfill the macroscopic dynamic equations derived from local conservation laws. The equations of interest are the equation of continuity, the equation for the flux (hydrodynamic equation) and the dynamic equations for energy, entropy. Phenomenological relations between flux and force are introduced. The microscopic basis for these equations has been investigated. The *Smoluchowski* equation provides the single particle probability function $f(r, t)$ (or with proper normalization the number density $n(r, t)$):

$$\frac{\partial f}{\partial t} = D\left[\frac{\partial}{\partial \boldsymbol{r}} \cdot \frac{\partial}{\partial \boldsymbol{r}} f + \frac{\partial}{\partial \boldsymbol{r}} \frac{u}{kT} \cdot \frac{\partial}{\partial \boldsymbol{r}} f + f \frac{\partial}{\partial \boldsymbol{r}} \cdot \frac{\partial}{\partial \boldsymbol{r}} \frac{u}{kT}\right]$$

D is the diffusion constant and u is an external potential (Doi and Edwards, 1986). The Smoluchowski equation is seen to be equivalent to Model B and to the equation of continuity if the probability flux is

$$\boldsymbol{j}(\boldsymbol{r}, t) = -Df \frac{\partial}{\partial \boldsymbol{r}} \left(\ln f + \frac{u}{kT} \right)$$

Brownian motion describes the dynamics of particles in an effective surrounding medium and provides a more detailed description by following the average motion in phase space, i.e. the evolution of the distribution $f(\boldsymbol{r}, \boldsymbol{v}, t)$ of velocity $\boldsymbol{v}$ as well as position $\boldsymbol{r}$. The theory is based on an expansion of the global probability and use of the Markov

relation (Rice and Gray 1965; Huang 1963). The classical description of the phase space dynamics follows the well-known differential equation, usually called the *Fokker Planck* (FP) equation:

$$\frac{\partial f}{\partial t} = \frac{\xi}{m}\left[3f + \frac{kT}{m}\frac{\partial}{\partial \boldsymbol{v}} \cdot \frac{\partial f}{\partial \boldsymbol{v}} + \boldsymbol{v}.\frac{\partial}{\partial \boldsymbol{v}} f\right] - \boldsymbol{v}.\left[\frac{\partial}{\partial \boldsymbol{r}} f\right] + \frac{1}{m}\frac{\partial u}{\partial \boldsymbol{r}} \cdot \frac{\partial}{\partial \boldsymbol{v}} f$$

Average properties of interest are calculated from the solution of the equation for the distribution in phase space $f(\boldsymbol{r}_0\boldsymbol{v}_0, \boldsymbol{r}\boldsymbol{v}t)$ for $\boldsymbol{r}, \boldsymbol{v}$ at t, fixing $\boldsymbol{r}_0, \boldsymbol{v}_0$ at $t = 0$:

– The average particle number density $n(\boldsymbol{r}, t)$ depends on the initial distribution f_i: $n(\boldsymbol{r}, t) = \int d\boldsymbol{r}_0\, d\boldsymbol{v}_0\, d\boldsymbol{v} f(\boldsymbol{r}_0\boldsymbol{v}_0, \boldsymbol{r}\boldsymbol{v}t) f_i(\boldsymbol{r}_0\boldsymbol{v}_0)$
– the average local particle velocity $\boldsymbol{v}(\boldsymbol{r}, t)$ at $\boldsymbol{r}$ after time t, $n(\boldsymbol{r}, t)\,\boldsymbol{v}(\boldsymbol{r}, t) = \int d\boldsymbol{r}_0\, d\boldsymbol{v}_0\, d\boldsymbol{v} f(\boldsymbol{r}_0\boldsymbol{v}_0, \boldsymbol{r}\boldsymbol{v}t) f_i(\boldsymbol{r}_0\boldsymbol{v}_0)\boldsymbol{v}$
– the kinetic stress tensor $\hat{\boldsymbol{T}}(\boldsymbol{r}, t) = \int d\boldsymbol{r}_0\, d\boldsymbol{v}_0 d\boldsymbol{v} f(\boldsymbol{r}_0\boldsymbol{v}_0, \boldsymbol{r}\boldsymbol{v}, t) f_i(\boldsymbol{r}_0\boldsymbol{v}_0)\boldsymbol{v}\boldsymbol{v}$
– the energy flux tensor $\hat{\boldsymbol{Q}}(\boldsymbol{r}, t) = \int d\boldsymbol{r}_0\, d\boldsymbol{v}_0\, d\boldsymbol{v} f(\boldsymbol{r}_0\boldsymbol{v}_0, \boldsymbol{r}\boldsymbol{v}, t) f_i(\boldsymbol{r}_0\boldsymbol{v}_0)\boldsymbol{v}\boldsymbol{v}\boldsymbol{v}$

An infinite set of coupled equations is obtained for the density $n(\boldsymbol{r}, t)$, the flux $\boldsymbol{j}(\boldsymbol{r}, t) = n(\boldsymbol{r}, t)\boldsymbol{v}(\boldsymbol{r}, t)$, the pressure tensor $\hat{\boldsymbol{T}}(\boldsymbol{r}, t)$, the energy flux $\hat{\boldsymbol{Q}}(\boldsymbol{r}, t)$ and so on, by an average in the distribution of momentum and in the initial conditions. A complete solution of such equations results in a continuum description of the average motion and can be compared to the macroscopic equations of irreversible thermodynamics.

The differential equations for the moments of f are found by multiplication of the FP equation by the nth rank tensor $\boldsymbol{v}\boldsymbol{v}\boldsymbol{v}\boldsymbol{v}, \ldots, \boldsymbol{v}$ and integration in momentum space with the condition that the surface terms in momentum space vanish for $\boldsymbol{v} \to \infty$. The kinetic equations thus obtained are similar to hydrodynamics and physically intuitive. Analogous methods of solution can be used.

$$\frac{\partial n}{\partial t} = -\frac{\partial}{\partial \boldsymbol{r}} \cdot \boldsymbol{j}$$

$$\frac{\partial \boldsymbol{j}}{\partial t} = -\frac{\xi}{m}\boldsymbol{j} - \frac{\partial}{\partial \boldsymbol{r}}\widehat{T} - \frac{n}{m} \cdot \frac{\partial}{\partial \boldsymbol{r}} u$$

$$\frac{\partial \widehat{T}}{\partial t} = -\frac{2\xi}{m}\widehat{T} + \frac{2\xi kT}{m^2} n\widehat{E} - \frac{\boldsymbol{j}}{m}\frac{\partial}{\partial \boldsymbol{r}} u - \frac{\partial}{\partial \boldsymbol{r}}\widehat{\boldsymbol{Q}}$$

$\widehat{E}$ is the unit tensor. For a large friction coefficient $\xi \to \infty$, it can be shown by subsequent replacement that these equations reduce to the Smoluchwski equation. The equation for the flux contains the macroscopic hydrodynamic equations when attenuation by friction with the surrounding environment is neglected. The set of equations can be truncated by neglect of the energy flux $\widehat{\boldsymbol{Q}}$ in fluids with low viscosity and use of the adiabatic approximation. Since $\widehat{\boldsymbol{T}}$ decays with a characteristic time $\tau/2$ and $\boldsymbol{j}$ with τ, $\widehat{\boldsymbol{T}}$ and $\boldsymbol{j}$ will have achieved the stationary values for $t \gg \tau = m/\xi$: the kinetic tensor of independent particles with an Boltzmann distribution of velocity $\hat{\boldsymbol{T}} = (\frac{nkT}{m})\hat{\boldsymbol{E}}$ and the flux $\boldsymbol{j} = -m/\xi\ [\mathrm{grad}\hat{\boldsymbol{T}} + n/m\ \mathrm{grad}\ u]$ due to the gradient of the local potential. The problem is then reduced to a calculation of the density from the resulting mesoscopic equation.

The *Boltzmann equation* attempts to go beyond mean field theory but the mesoscopic equations, after averaging in velocity, are identical to those of the Fokker Planck equation.

A *generalized Fokker Planck* equation can be used to describe the kinetics of any system parameter η, which can be scalar, vector, tensor or combination of these (de Groot, Mazur, 1962). Define $P(\eta\eta', t)$ as the probability to find η' at time t if η was found at $t=0$, then $P(\eta\eta', t)$ should satisfy

$$\frac{\partial P}{\partial t} = Q\left[\frac{\partial}{\partial \eta}\frac{\partial P}{\partial \eta}\right] - \left[\frac{\partial}{\partial \eta} P \cdot U\right]$$

The coefficients are correlation functions, in $\Delta\eta = \eta' - \eta$ which must be derived or modeled.

$$U = \lim_{t\to 0}\frac{1}{t}\int d\eta'\, \Delta\eta P(\eta, \eta', t)$$
$$2Q = \lim_{t\to 0}\frac{1}{t}\int d\eta'\, \Delta\eta\, \Delta\eta P(\eta, \eta', t)$$

An exact solution of this equation is difficult and has been possible only in special cases such as the field free case and for a harmonic force field.

The *generalized Langevin equations* are an equivalent description of the Fokker Planck equation. An equation of motion similar to that of classical mechanics is used as a starting point:

$$\frac{\partial \eta}{\partial t} = M(\eta) + \varepsilon(t)$$

The generalized force is $M(\eta)$. For example the harmonic force is often used with $M(\eta) = -\Gamma\eta$. The term ε(t) represents the random force of the surrounding medium and must fulfill the set of requirements which describe a random variable. From this equation, all average moments of η can be calculated for a given force field and thus ultimately, the probability distribution. Classical FP follows from the Langevin equations of motion for the variables $\boldsymbol{r}$ and $\boldsymbol{v}$

$$\frac{\partial \boldsymbol{v}}{\partial t} = -\frac{\xi}{m}\boldsymbol{v} - \frac{1}{m}\frac{\partial u}{\partial \boldsymbol{r}} + \varepsilon(t)$$
$$\frac{\partial \boldsymbol{r}}{\partial t} = \boldsymbol{v}$$

6.4. From Microscopic to Mesoscopic

Atomic scale dynamic theories and numerical simulation explore atomistic processes and follow the movement of individual atoms. In the final result, averages are produced over a series of "measurements" made as the system evolves. The relevant physics folds atomistic understanding into a mesoscopic formulation. Collective behavior can be captured on this scale and embedded in a continuum mechanics approach. In simulations by molecular dynamics, the trajectory of a particle is followed in time (Allen and Tidesley, 1995; Rapaport, 1995). The dynamics are not deterministic far from equilibrium, any path is possible and the system is dominated by random fluctuations. The problem is similar to the statistics for the conformation of a polymer chain which follows from a distribution around a minimum of the total energy. The chain can represent

a path, the monomer distance a time and assumptions made on the most probable trajectory of a particle (Edwards, 1965; de Gennes, 1969). Simple diffusion follows from a Gaussian distribution of steps around an average fixed length (compare Section 3). A more complete description of the kinetics investigates the momentum as well as the position (ten Bosch, 1999, 2003). A kinetic equation for the probability $f(\boldsymbol{r}, \boldsymbol{v}, \boldsymbol{r}_0, \boldsymbol{v}_0, t)$ to find a particle with a given velocity and position at a given time for given initial conditions can be derived from the Gauss distribution around the most probable path. The equation which results is not identical to the classical Fokker Planck equation except in the field free case.

The mean field between particles $u(r)$ is included and paths are distributed close to those of constant energy. As was shown in equilibrium theory, the best choice appears to be given by the change of the internal energy U on changing the local density $n(r, t)$ or $u(r) = \delta U/\delta n$. By definition $u(r) = \delta(F - F_{\mathrm{id}})/\delta n$ where F is the free energy and F_{id} the ideal free energy, or $u(r) = \mu(r) - kT \ln n(r)\Lambda$ with $\mu(r)$ the local chemical potential of DFT. Thus, to lowest order, the average interaction is given by the direct correlation function (see Section 2.2). The driving force for the dynamics of the nonequilibrium system is the gradient of the local chemical potential, a functional of the local particle density derived from equilibrium DFT models. Once local and transient effects have expired and the inertial terms become negligible, the dynamics of model B are recovered and this can be shown for FP as well. The equilibrium distribution is obtained for $\mathrm{grad}\, \mu(r) = 0$. As expected from themodynamics, the chemical potential is a constant and the results of the previous chapters are confirmed.

The connection to model A is related mainly to the conservation or not of energy along a trajectory.

6.5. Dynamic Phenomena

The crucial question is access to nonequilibrium properties. Equilibrium DFT has withstood the test of time but a firm basis for the dynamics is still being explored. A short description of major problems that are still outstanding follows.

–Does a constant velocity profile exist?

The kinetic equations are complex nonlinear partial differential equations. A solution of the form $n(r, t) = n(\boldsymbol{r} - \boldsymbol{R}(t))$ if it exists simplifies the mathematics. The variation of the profile front $\boldsymbol{R}(t)$ is obtained from the kinetic equation by using the relation $\partial n/\partial t = -\partial n/\partial \boldsymbol{r}\, d\boldsymbol{R}/dt$ or from conservation of particle number. A variational procedure for the fastest growing front has also been used (San Miguel *et al.*, 1981).

The "soliton" solution requires the density profile to translate uniformly without deformation and does not lead to contradictions within the assumptions of model A. However, in model B, the equilibrium profile cannot be used since the flux vanishes and more generally, the local chemical potential is a strong function of position.

–How to describe the dynamics of phase transitions?

It was shown in Section 3 that for certain external conditions, two phases can coexist. If an uniform sample is prepared within the zone of coexistence of the phase diagram, the initial metastable phase will disappear and be replaced by the stable phase (Landau and Lifshitz, 1970). The order parameter profile evolves with time until the conditions of equilibrium are met with two phases separated by a stationary profile of constant chemical potential. The kinetics of the phase transition have been described using

various model approaches (Gunton *et al.*, 1983). Nucleation and growth on a substrate is reviewed in Zinke Allmang *et al.*, 1992.

–Existence of a critical droplet?
Capillary pressure stabilizes a curved surface at a certain radius a_c (Talanquer and Oxtoby, 1996). This equilibrium solution was suggested to appear in the dynamics of droplet growth as the critical radius for which no growth or decay occurs and therefore as a stationary solution of the kinetic equations.

The profile of the liquid droplet is calculated from an equation of the form $(da/dt) = -\Gamma(\delta F/\delta a)$ where $F(a)$ contains an surface term in a^2 which inhibits cluster growth and a volume term in a^3 which is favorable to growth. A balance occurs for the critical radius with $da/dt = 0$ (Mouti and ten Bosch, 1993). The role of the critical droplet in cluster growth is still being explored. In the scenario of Oswald ripening, clusters of radius $a > a_c$ can grow but clusters of radius $a < a_c$ must decay due to the unfavorable surface to volume ratio if the profile shape is to remain unchanged on propagation.

–Spinodal decomposition and other instabilities?
In nucleation and growth during a phase transition, the morphology of the process was observed to depend on the position of the initial phase in the phase diagram. Along the binodal, coexistence between two phases occurs and for given external parameters, two values of the order parameter. For a point inside the binodal, the uniform system is not thermodynamically stable and phase separation takes place by layer or cluster growth. It was suggested that a further limiting line exists, the spinodal (Langer, 1980). If inside this region, the system is thermodynamically unstable then $d^2F/dn^2 < 0$. For model *B*, standard linear stability theory yields an instability of a periodic density perturbation. The dynamics follow the Cahn Hilliard model (Walgraef, 1996)

$$\frac{\partial n}{\partial t} = \Gamma \frac{\partial^2}{\partial x^2}\left[\frac{\mu(n(x))}{kT} - \kappa \frac{\partial^2}{\partial x^2} n\right]$$

Growth of the new phase would therefore not occur by layers or clusters, with increase in extent and no change in density but rather by periodic domains which increase in amplitude and wave length. Similar results can be extended to other order parameters and ensue from other models. The reality of the spinodal is based on the possibility of thermodynamically unstable phases and is still being questioned (Binder and Stauffer, 1976). Experiments and numerical simulation are not conclusive.

7. CONCLUSIONS

An analytical theory is useful in applied science as it is detached from a given specific material or phenomenon, unlike numerical simulation. Successful mapping from an atomistic model to a mesoscale model preserves only certain aspects of relevance and has the advantage that time and length scales become accessible beyond those of atomistic simulations. For example, the single bond vibrations in a polymer chain vary in a time 10^{-13} s and space 10^{-8} cm and these motions are not important for flow in a polymer solution. Multiscale modeling (Diaz de la Rubia and Bulatov, 2000) combines these ideas as well as analytical and numerical analysis to form a powerful tool for the study of materials.

Acknowledgment

My grateful thanks to Prof V. Sterligov for the figures.

References

Allen, M.P. and Tildesley, D.J. (1995). *Computer Simulations of Liquids*. Clarendon Press, Oxford.
Binder, K. and Stauffer, D. (1976). *Adv Phys.*, **25**, 343.
Chandrasekhar, S. (1943). *Rev Mod Phys.*, **15**, 1.
Chen, X.J., Levi, A. and Tosatti, E. (1991). *II Nuovo Cimento*, **13**, 919.
Diaz de la Rubia, T. and Bulatov, V. (Eds.) (2001). *MRS Bulletin* **26/3**, 169.
Dietrich, S. (1991). *Phase Transitions in Surface Films*. Plenum Press, N.Y.
Doi, M. and Edwards, S.F. (1986). *Theory of Polymer Dynamics*. Clarendon Press, Oxford.
Edwards, S.F. (1965). *Proc. Royal Soc.*, **85**, 613.
Evans, R. (1979). *Adv. Phys.*, **28**, 143.
Flory, P. (1953). *Principals of Polymer Chemistry*. Cornell, Ithaca.
Foiles, S.M. (1996). *MRS Bulletin* **21/2**, 17.
Frisch, H. and Lebowitz, J.L. (1964). *Theory of Classical Fluids*. W.A. Benjamin, N.Y.
de Gennes, P.G. (1969). *Rep. Prog. Phys.*, **32**, 187.
de Gennes, P.G. (1979). *Scaling Concepts in Polymer Physics*. Comell, Ithaca N.Y.
de Gennes, P.G. (1985). *Rev. Mod. Phys.*, **57**, 827.
de Groot, S.R. and Mazur, P. (1962). *Non-equilibrium Thermodynamics*. North Holland, Amsterdam.
Guggenheim, E.A. (1952). *Mixtures*. Clarendon Press, Oxford.
Gunton, J.D., San Miguel, M. and Sahmi, P. (1983). *Phase Transitions and Critical Phenomena*, **8**, 269. Academic Press, London.
Hill, T.L. (1962). *Introduction to Statistical Thermodynamics*. Addison Wesley, Reading.
Hohenberg, P.C. and Halperin, B.I. (1977). *Rev. Mod. Phys.*, **49**, 435.
Hong, K. and Noolandi, (1981). *Macromolecules*, **14**, 727.
Huang, K. (1963). *Statistical Mechanics*, J. Wiley, N.Y.
Isrealachvili, J. (1992). *Intermolecular and Surface Forces*. Academic Press, San Diego.
Jeröme, B. (1991). *Rep. Prog. Phys.*, **54**, 392.
Labastie, P. and Whetten, R.L. (1990) *Phys. Rev. Letters*, **65**, 1567.
Landau, L.D. and Lifshitz, I.M. (1970). *Course of Theoretical Physics 10*. Pergamon Press, Oxford.
Langer, J.S. (1971). *Ann. of Phys.*, **65**, 53.
Langer, J.S. (1980). *Rev. Mod. Phys.*, **52**, 1.
Lifshitz, I.M., Grosberg, A. and Khokhlov, A. (1978). *Rev. Mod. Phys.*, **50**, 683.
Löwen, H. (1994). *Physics Reports*, **237**, 249.
Lubensky, T.C. (1970). *Phys Rev.*, **A2**, 2497.
McMullen, W. and Freed, K.F. (1990). *J. Chem. Phys.*, **92**, 1413.
Montroll, E.W. and Lebowitz, J.L. (1987). *Fluctuation Phenomena*. North Holland, Amsterdam.
Mouti, M. and ten Bosch, A. (1993). *J. Chem. Phys.*, **99**, 1796.
Ohring, M. (1992) *The Materials Science of Thin Films*, Academic Press, San Diego.
Oxtoby, D.W. (1991). *Liquids Freezing and the Glass Transition*. Elsevier, Amsterdam.
Priestley, E.B., Wojtowitz, P.J. and Sheng, P. (1975). *Introduction to Liquid Crystals*. Plenum Press, N.Y.
Rapaport, D.G. (1995). *The Art of Molecular Dynamics Simulation*. University Press, Cambridge.
Rice, S.A. and Gray, P. (1965). *Statistical Mechanics of Simple Liquids*. Interscience, N.Y.
Ronca, G. and ten Bosch, A. (1991). *Liquid Crystallinity in Polymers*, J. Wiley, New York.
San Miguel, M., Gunton, J.D., Dee, G. and Sahni, P. (1981). *Phys. Rev.*, B **23**, 2334.
Singh, Y. (1991). *Phys. Reports*, **207**, 351.
Somorjai, G.A. (1998). *MRS Bulletin May*, 11,
Stephen, M. and Straley, J.P. (1974). *Rev. Mod. Phys.*, **46**, 617.
Sullivan, D.E. and Telo da Gama, M.M. (1986). *Fluid Interfacial Phenomena*. J. Wiley, N.Y.
Talanquer, V. and Oxtoby, D.W. (1996). *J. Chem. Phys.*, **104**, 1483.
Tarazona, P. and Evans, R. (1983). *Mol. Phys.*, **48**, 799.
Telo da Gama, M.M. (1984). *Mol. Phys.*, **52**, 585.
ten Bosch, A. (1999). *Physica A* 262, 396; *Phys. Rev. E* (2003).
Vroege, G.J. and Lekkerkerker, H. (1992). *Rep. Prog. Phys.*, **55**, 1241.
Walgraef, D. (1996). *Spatio-Temporal Pattern Formation*. Springer (N.Y.).
Widom, B. (1991). *Liquids Freezing and the Glass Transition*. Elsevier. Amsterdam.
Yamakawa, H. (1971). *Modern Theory of Polymer Solutions*. Harper and Row, N.Y.
Zinke Allmang M., Feldman, L. and Grabow, M. (1992). *Surf. Sci. Rep.*, **16**, 377.